The State of Libya

University of Zawia

Faculty of Science

Department of Chemistry

Synthesis and characterization of 4-amino antipyrin derivatives and their metal complexes

Submitted By:Maryam Aboulqasim Abdulsalam Alsabbani

Supervisor: Dr-Salem Kalefa El-fared

Doctor in In organic chemistry

Thesis Was Submitted in Partial Fulfillment of The Requirements for The

Degree of Master in Science in Chemistry.

…./…/2025

جامعة الزاوية

كلية العلوم – قسم الكيمياء

تحضير ودراسة وتوصيف مركبات 4-أمينوأنتيبايرين ومعقداتها المعدنية

مقدمة من: مريم ابوالقاسم عبد السلام السباني

بكالوريوس علوم (كيمياء)

اشراف: د. سالم خليفة الفرد

أستاذ الكيمياء الغير عضوية

الرسالة مقدمة إلى قسم الكيمياء كلية العلوم – جامعة الزاوية لإستيفاء الحصول على درجة الماجستير

في العلوم (الكيمياء)

ملخص الرسالة

تُعد قواعد شيف التي تحتوي على ذرات مانحة من النيتروجين والأكسجين من المركبات الواعدة في العديد من المجالات، مثل الحفز الكيميائي، والكيمياء التحليلية، وعلوم المواد. و يهدف هذا البحث إلى تحضير ودراسة الخواص التركيبية والطيفية لمعقّد نحاس ثنائي التكافؤ مشتق من ليجاند قاعدة شيف ناتج عن تفاعل تكاثف بين مركب 4–أمين أنتيبايرين ومركب الساليسيالدهيد حيث تم الحصول على الليجاند (ساليساليدين أمينوأنتيبايرين) وهو مركب عضوي يحتوي على مجموعة آزوميثين ومجموعة فينولية ، ولاحقا تم تنسيقه مع كلوريد النحاس باستخدام طريقة ثنائي الطور التي تشمل مذيب عضوي (التولوين) ووسطاً مائياً. أجريت عملية التوصيف باستخدام عدد من التقنيات، شملت التحليل الطيفي بالأشعة تحت الحمراء، والتحليل الطيفي في المجال المرئي وفوق البنفسجي، وقياس الموصيلية المولارية، واختبارات الذوبانية، إضافة إلى دراسة حيود الأشعة السينية للأحادي البلورة. أظهرت النتائج أن الليجاند يتفاعل مع النحاس عبر ذرتي النيتروجين من مجموعة الآزوميثين والأكسجين من المجموعة الفينولية، مما يؤكد طبيعته ثنائية السن في التنسيق. كما بينت التحاليل الطيفية وجود انتقالات إلكترونية تدل على تكوين معقّد ذي هندسة مربعة مستوية حول مركز النحاس، وقد أكدت نتائج حيود الأشعة السينية أن البنية البلورية للمعقّد تتخذ شكلاً مربعاً مستوياً مشوّهاً، تثبته روابط هيدروجينية وتفاعلات بين الحلقات العطرية. كما أظهر المعقّد قابلية جيدة للذوبان في المذيبات العضوية القطبية، وسلوكاً غير إلكتروليتي، مما يشير إلى طبيعته الجزيئية المتعادلة. وتبرز هذه النتائج إمكانيات قواعد شيف المعتمدة على مركب 4–أمينو أنتيبايرين في تنسيق الفلزات الانتقالية، مما يفتح آفاقاً لتطبيقات مستقبلية في مجالات الحفز الكيميائي والكيمياء الحيوية غير العضوية.

Abstract

N, O- donor Schiff bases and their metal complexes have potential applications in fields like catalysis, analytical chemistry, and materials science. This study reports the synthesis, structural characterization, and spectroscopic analysis of a copper(II) complex derived from a Schiff base ligand formed via condensation of 4-aminoantipyrine and salicylaldehyde. The resulting ligand, Salicylidene Amino Antipyrine, was successfully complexed with $CuCl_2$ using a biphasic method involving toluene and aqueous media. Characterization techniques including FT-IR, UV-Vis spectroscopy, molar conductivity, solubility testing, and single-crystal X-ray diffraction (SCXRD) confirmed the bidentate coordination of the ligand via azomethine nitrogen and phenolic oxygen atoms. Spectral data revealed $\pi \rightarrow \pi^*$, $n \rightarrow \pi^*$, and d–d transitions consistent with square planar geometry around the Cu(II) center. The SCXRD analysis confirmed a distorted square planar configuration, stabilized by hydrogen bonding and π-stacking interactions. The complex exhibited good solubility in polar organic solvents, indicating a neutral molecular nature. The findings underscore the structural versatility and coordination potential of 4-aminoantipyrine-based Schiff bases for transition metal complexation, with implications for future applications in catalysis and bioinorganic chemistry.

Key words:

4-Aminoantipyrine, salicylaldehyde, Copper (II)complex, SC-X-ray diffraction.

DECLARATION

I, Maryam Aboulqasim Abdulsalam Alsabbani, confirm certify that the work presented in this thesis, "Synthesis and Characterization of 4-Amino Antipyrine derivatives and Their Metal Complexes," is my own original research, conducted in partial fulfillment of the requirements for the degree of Master of Chemistry Science at the University of Zawia. I confirm that all sources have been properly acknowledged and referenced and that this thesis has not been submitted for any other degree or professional qualification. I furthermore cede copyright of this thesis in favor of the University of Zawia.

Student name: .....

Signature: .....

Date: ..... / ...../ 20

Dedication

To the souls of my father and mother, may God have mercy on them and forgive them.

To them, I dedicate this achievement in gratitude and appreciation.

To my husband and children, who have been a source of inspiration and motivation for me to continue.

And to everyone who has contributed to this achievement.

To my distinguished teachers.

ACKNOWLEDGEMENT

All praise and thanks be to Allah, whose blessings and guidance enabled me to complete this thesis.

I would like to extend my sincere thanks to my ***professor,D. Salem El-Fared,*** for his valuable assistance and supervision throughout the dissertation. I also extend my sincere thanks to ***Professor, D. Hussain Al-Arabi*** for his scientific support and academic guidance. I also *thank Ms. Mariam Saleh* for their support. I would also like to thank the Tajoura Plastics Research Center for providing **FT-IR** analysis, as well as *Dr. Carla* from the University of Lisbon for facilitating the sample analysis by **SCXRD** technique.

Finally, I am deeply grateful to my family for their endless love, support, and encouragement throughout this journey.

LISTE OF CONTAIN

LIST OF TABLES

LIST OF FIGURES

LISTE OF SCHEMES

LIST OF APPENDIX

LIST OF SYMBOLS AND ABBREVIATIONS

ABBREVIATION	MEANING
IUPAC	International Union of Pure and Applied Chemistr
IR	infrared
UV	Ultra Violet
NMR	Nuclear Magnetic Resonance
MS	Mass spectrometry
EPR	Electron Paramagnetic Resonance
SCXRD	Single Crystal X-ray Diffraction
FT-IR	Fourier-Transform Infrared
SEM	Scanning Electron Microscopy
EDX	Energy Dispersive X-ray spectroscopy
TGA	Thermo Gravimetric Analysis
DTA	Diffefential Thermal Analysis
MCF	Michigan Cancer Foundation
DFT	Density Functional Theory
HOMO	Highest Occupied Molecular Orbital
LUMO	Lowest Unoccupied Molecular Orbital
4AAP	4-amino antipyrine
EtOH	Ethanol
TLC	Thin layer chromatography
SAAP	Salicylidene amino antipyrin
SHELXD	Structure solution using Heavy atoms
SHEL XL	SHELX Refinement Program
DSC	Differential Scanning Calorimetry

ESI-MS	Electrospray Ionization Mass Spectrometry
ITIES	Ion Transfer Across Immiscible Electrolyte Solutions
M.P	Melting point
W	Weight
mmol	Milli mol
g	Gram
ml	Milli liter
Å	Angstrom
B, γ, α	Beta,Gama,Alpha
k	Kelvin
Cm^{-1}	Centimeter

CHAPTER I:
INTRODUCTION

1- Introduction:

Schiff bases were first introduced in the 19th century by German Chemist Hugo Schiff, who described them as the products of condensation reactions between primary amines and carbonyl compounds, highlighting their unique properties and reactivity. In 1864, Hugo Schiff synthesized Schiff bases through azeotropic distillation, using an aldehyde or ketone and a primary amine [1-6]. In the years after Schiff's pioneering discovery, chemists explored the principles behind Schiff bases more thoroughly. Prominent figures like Emil Fischer made significant contributions by broadening the variety of Schiff base reactions and offering insights into their stereochemistry [7, 8]. Now a day's Chemists are increasingly interested in Schiff bases that come from heterocyclic rings, using carbonyl compound as a key focus in various fields such as biology, medicine, clinical studies, analytics, and pharmacology [9].

1.1-Chemistry of Schiff base

Schiff bases are a group of organic compounds formed through the condensation reaction between a primary amine (-C=N-) and a carbonyl compound, usually an aldehyde or ketone, with the elimination of water [7]. Schiff bases are defined by a central carbon-nitrogen double bond, referred to as an imine or azomethine group, which forms during the reaction, with the general structure $R_1R_2C{=}NR'$ (where $R' \neq H$) [1-7]. Schiff bases are a type of imine where R′ is an alkyl aryl or heterocyclic groups (not hydrogen), while R1 and R2 can be hydrogen [6, 9] (Figure 1.1 and 1.2). Depending on their structure, they may be considered secondary aldimines or secondary ketimines [7].

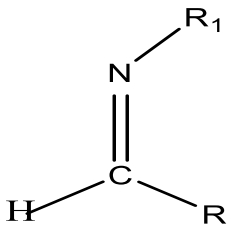

Figure 1.1: General Structure of Schiff Base

According to IUPAC guidelines, Schiff bases are defined as chemical compounds (imines) that contain a hydrocarbyl group attached to the nitrogen atom [10]. In synthetic chemistry, Schiff bases are commonly known as imines or azomethine groups [11, 12]. While, in coordination

chemistry, Schiff bases are common ligands, which are derived from aromatic aldehydes and alkyl diamines [13].

Schiff bases are versatile compounds with a rich structural chemistry. The imine linkage, along with the nature of the substituents, plays an essential role in determining their reactivity, stability, and potential applications in various fields, including coordination chemistry [6, 7]. The most major feature of Schiff bases is the imine group, where the nitrogen atom is double-bonded to a carbon atom [14]. This bond is highly polar, with the nitrogen atom being more electronegative than carbon, results in partial charges that impact the compound's reactivity and interactions [14, 15].

Schiff bases are of significant importance in the fields of chemistry and materials science because of their unique properties such as versatility, simplicity, and functionality [15]. The properties of Schiff bases can vary widely depending on the nature of the substituents involved, impacting their stability, solubility, and reactivity. Where, these properties are influenced by both steric and electronic effects of the substituents [14-16].

For instance, electron-donating groups (such as alkyl groups) make the nitrogen more nucleophilic, while electron-withdrawing groups (such as halogens) stabilize the Schiff base by delocalizing the electron density [17-19]. In addition, structural stability and reactivity of Schiff base can be affected by hydrogen bonds which can form when hydroxyl groups are present in the substituents [19]. The type and position of these substituents can modify hydrogen bonding interactions, thus affecting the properties of Schiff bases [18]. These compounds are often crystalline solids, weakly basic, and can form insoluble salts with strong acids. Schiff bases serve as intermediates in the synthesis of amino acids and as ligands for the preparation of metal complexes with several structures [19, 20]. The imine group (-C=N-), which is highly reactive can form various complexes with metal ions. Thus, Schiff bases are one of the most widely used as chelating ligands in coordination chemistry [20].

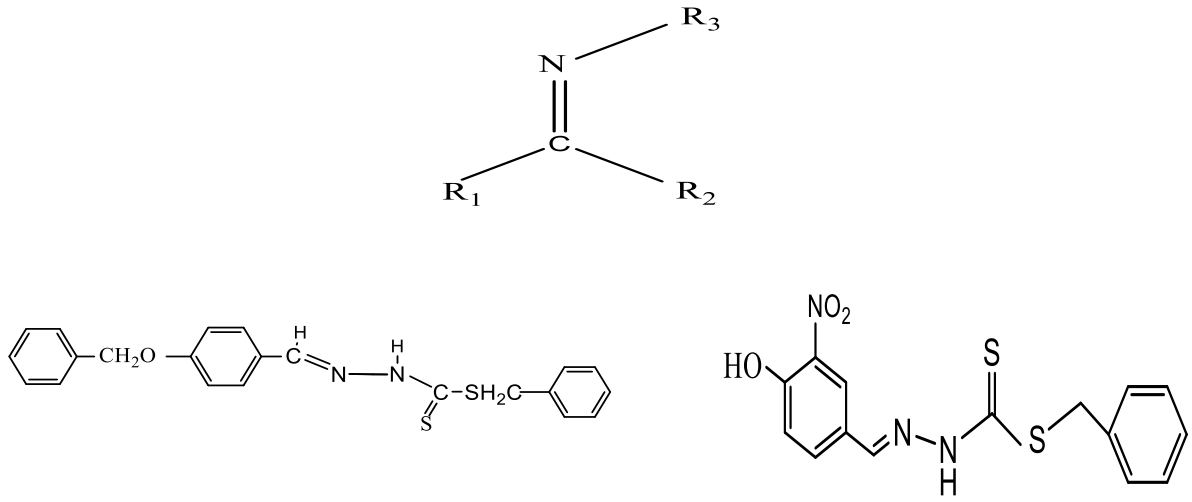

Figure1. 2: General Structure of Schiff bases with examples

1.2- Structural and Coordination Chemistry

In coordination chemistry, Schiff bases as ligands have been widely studied because of their ability, versatility and capacity to form stable complexes with transition metals, prompting extensive research into their synthesis, characterization, and several applications [21, 22]. N, O- donor Schiff bases and their metal complexes have potential applications in fields like catalysis, analytical chemistry, and materials science, including magnetic and photoluminescent materials [22].

The coordination chemistry of Schiff base metal chelates has been recognized for over a century. Schiff bases, as ligands, are classified based on the number of donor atoms they possess, such as mono-, bi-, tri-, and tetradentate ligands [14]. These ligands are highly reactive due to the presence of lone pairs on their sp^2 hybridized atoms [19- 22]. The nitrogen and oxygen atoms in Schiff bases interact with metal centers, influencing the coordination environment and reactivity of the metal. In addition, Schiff bases often contain additional functional groups, like hydroxyl (–OH), amine ($–NH_2$), or thiol (–SH) groups, which enable them to function as multidentate donors [21].

These ligands readily form stable complexes with metal ions in various oxidation states, such as bidentate and tridentate complexes with Co(II) and Ni(II), or even tetradentate complexes with metal ions like Ni(II), Cu(II), Pd(II), and higher oxidation states such as V(IV), Ti(IV), and U (III, IV, V) [21].

The nitrogen and oxygen atoms of Schiff bases interact with metal ions through their lone pairs of electrons, coordinating to the metal center. This coordination can occur through diverse

geometries depending on the nature of the Schiff base and the metal ion involved [19, 23]. The number of coordination sites occupied by the Schiff base ligand can differ depending on the metal's coordination preferences, which are influenced by the electronic configuration and the ionic radius of the metal [15, 24].

As above-mentioned, Schiff bases are classified based on the number of donor atoms that can coordinate to the metal center:

- **A monodentate Schiff base** binds to a metal center via a single donor atom (usually nitrogen) donating a single pair of electrons to form a coordination bond with metal ions. The bonding interaction is typically polar, where the nitrogen atom, being more electronegative than carbon, donates electron density to the metal center [25]. The metal ion forms a stable complex with the Schiff base ligand depending on its oxidation states. The geometry of the complex can differ depending on the metal and its coordination number, with common geometries being tetrahedral, square planar, or octahedral. For coordination number 4, the complex often adopts a tetrahedral or square planar geometry. While for coordination number 6, the complex typically adopts an octahedral geometry, where six ligands surround the central metal ion in a symmetrical arrangement [26]. The Schiff base ligand's substituents, metal's size and charge, can significantly affect the geometry, stability, and reactivity of the complex [25].

The stability of a monodentate Schiff base complex is affected by the electronic properties of the Schiff base [25, 26]. Substituents that donate electron density to the metal such as hydroxyl groups could increase the stability of the complex, whereas electron-withdrawing groups could destabilize it [18].

N-salicylidene-ethylenediamine (where "salicylidene" refers to the salicylaldehyde derivative) is an example of Schiff base that can coordinate to a metal ion such as Cu^{+2} forming monodentate complex. In this example, the geometry around the metal ion could be square planar. The Schiff base will typically form a monodentate complex through nitrogen, with the metal ion possibly having coordination with additional ligands like chloride ions or water molecules (Figure 1.3) [26,27].

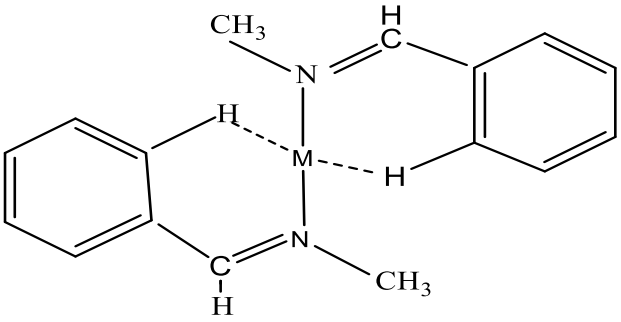

Figure 1.3: Structure of A monodentate Schiff base

- **Bidentate and tridentate Schiff bases** donate two pairs or three of electrons. These ligands usually have two functional groups that can donate lone pairs of electrons to the metal ion, forming two coordination bonds [23]. Typically, these donor atoms are the nitrogen of the imine group (C=N) and another atom like oxygen or nitrogen from a hydroxyl or amine group attached to the ligand [23-25]. Bidentate Schiff base ligands often form stable five- and six-membered chelate rings with divalent metal ions such as Ni^{2+}, Cu^{2+}, Co^{2+}, and Fe^{2+}.This chelation significantly increases the stability of the metal complex because of the chelate effect. Chelation enhances the stability of the complex due to the formation of multiple bonds between the ligand and the metal ion [26]. An example of a bidentate Schiff base legend is Salicylideneamine. This legend contains a hydroxyl group and an imine group, and both nitrogen and oxygen atoms coordinate to the metal ion, creating a stable chelate (Figure 1.4) [28].

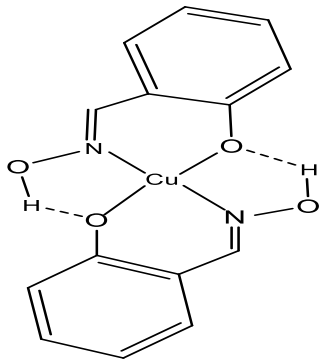

Figure 1.4: Structural of Copper (II) complex of the Schiff base ligand salicylaldoxime

The geometry around the metal ion in a bidentate Schiff base complex depends on the coordination number (typically 2, 4, or 6). If the metal is coordinated by just two donor atoms

(i.e., a simple bidentate Schiff base), the complex will likely adopt a linear geometry (180° bond angle). This is more common for metals like silver (Ag) or copper (Cu) in certain oxidation states (such as +1) [29]. While, if the coordination number is 4, the most common geometry would be tetrahedral or square planar. In tetrahedral geometry, the Schiff base ligand coordinates to metal ion in a way where the metal ion is at the center of a tetrahedron. This can occur with metals such as Zn(II) or Cu(II) (Figure 1.5) [27-30].

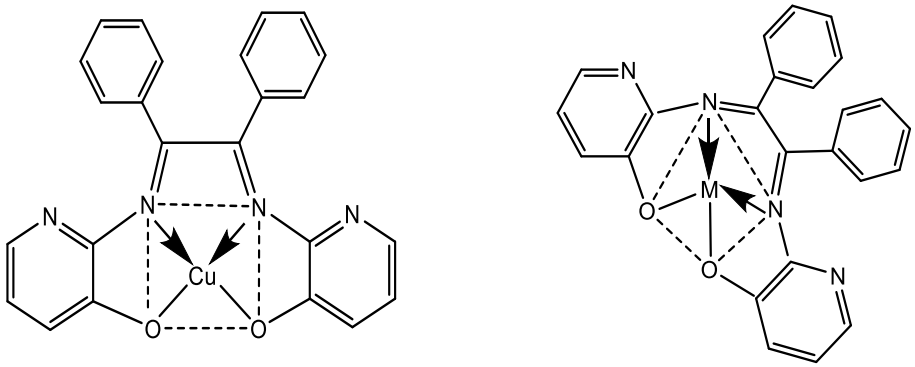

square planar geometry tetrahedron geometry

Figure 1.5: Structural formula of the complexes with coordination number 4

For metals with a coordination number of 6, such as Co(III), Fe(III), and Cr(III), the metal complex generally assumes an octahedral geometry. In this configuration, the bidentate Schiff base ligand typically occupies two of the six. For metals with a coordination number of 6, such as Co(III), Fe(III), and Cr(III), the metal complex generally assumes an octahedral geometry. In this configuration, the bidentate Schiff base ligand typically occupies two of the six available coordination sites, while the remaining positions are filled by other ligands, such as water, halides, or other anions (Figure 1.6) [31]

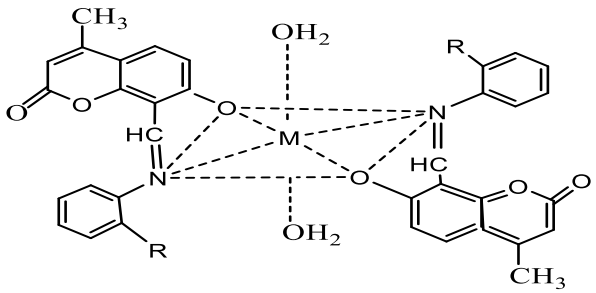

R=Cl & CH_3; M= Co (II), Ni (II) and Cu (II)

Figure 1. 6: Structural formula of the complexe having formula of Octahedral Geometry

- **Tridentate Schiff base** has three functional groups that each donate a lone pair of electrons to the metal ion, creating a chelate with the metal. The donor atoms can consist of nitrogen (from the imine group or amine), oxygen (from hydroxyl or carboxyl groups), or other heteroatoms capable of coordinating with the metal center [32]. The functional groups attached to the Schiff base impact the electron density and availability of lone pairs for coordination. The lone pairs of electrons from donor atoms (usually nitrogen and oxygen) form covalent bonds with the metal ion [33]. A common example of tridentate Schiff base is N, N'-bis(salicylidene) -1,2-diaminoethane, where two imine groups (-C=N-) and one hydroxyl group (-OH) provide three donor atoms (two nitrogens and one oxygen) to coordinate with the metal ion [33].

The coordination geometry of a tridentate Schiff base complex is influenced by both the coordination number of the metal ion and the structural characteristics of the Schiff base ligand. For tridentate Schiff base complexes, the coordination number of the metal is typically 4 or 6, depending on the metal's electronic configuration and the steric properties of the ligand [32, 33]. The coordination geometries of coordination number 4 are square planer and tetrahedral. In square planer geometry, the tridentate Schiff base ligand coordinates to the metal ion via three donor atoms, with the fourth coordination site often occupied by a solvent molecule or halide ion [33].

When it comes to tetrahedral geometry, the tridentate Schiff base ligand coordinates to the metal ion in a way that the donor atoms (nitrogen and oxygen) occupy four corners of a tetrahedron [32].

The geometry of coordination number 6 is octahedral. In this geometry, the tridentate Schiff base ligand coordinates with the metal through three donor atoms, occupying three coordination sites. The remaining three coordination sites are usually occupied by other ligands, such as water molecules, halides, or other anions [34]. In the octahedral geometry, the metal ion is at the center. Metal ions such as Fe^{2+}, Fe^{3+}, Co^{2+}, Cu^{2+}, and Cr^{3+} typically form octahedral complexes with six coordination sites [32- 34].

Tetradentate Schiff base ligands are multidentate compounds with four donor atoms, usually nitrogen and oxygen, that coordinate with a metal ion to form stable complexes. These ligands create four-membered chelate rings, donating four electrons to the metal center, which enhances stability, especially with metals like nickel (Ni^{2+}), copper (Cu^{2+}), and palladium (Pd^{2+}) that prefer four coordination sites [35]. The resulting complexes can adopt various geometries, such as octahedral, tetrahedral, or square planar, depending on the metal and ligand characteristics [36]. In the coordination of tetradentate Schiff base with metal ion, two donor atoms may come

from the imine (–C=N–) nitrogen atoms, while the other two donor atoms may come from other functional groups, such as hydroxyl (-OH), ether (-O-), or phenolic groups (-OH) attached to the ligand backbone. The remaining two coordination sites may be occupied by solvent molecules or other ligands [35, 36].

A common example of a tetradentate Schiff base ligand is the salen ligand (N, N' ethylenebis(salicylideneiminato)), which is created by reacting salicylaldehyde with ethylenediamine. This ligand can bind to a metal ion, such as copper(II), forming a complex with an octahedral structure [37].

1.3- Synthesis and characterization

Schiff bases are generally bi- or tridentate ligands capable of forming very stable complexes with transition metals. Schiff bases are compounds that contain an azomethine group (-HC=N-), formed through the condensation of aldehydes or ketones and primary amines, resulting in the elimination of water (Scheme 1.1). First discovered by Hugo Schiff in 1864, their formation typically occurs under acidic or basic conditions or with heat, a process known as the Schiff condensation [17]. The Schiff condensation, a process in which a primary amine attacks the carbonyl carbon of an aldehyde or ketone, forms a tetrahedral intermediate, which then undergoes dehydration to yield the imine linkage (C=N), producing the Schiff base [7, 17, 38]. Aldehydes create Schiff base ligands more easily than ketones. Aromatic aldehydes, particularly those that have strong conjugation systems, produce stable Schiff bases. On the other hand, aliphatic aldehydes tend to be unstable and disposed to polymerization.

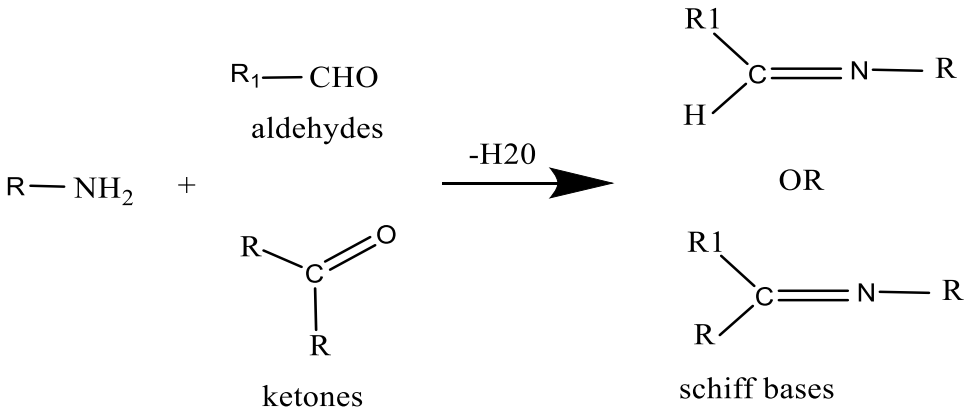

R1, R2 and / or R3 alkyle or aryle

Scheme 1.1: Synthesis of Schiff base

Schiff base metal complexes are characterized using a combination of analytical and spectroscopic techniques to confirm the structure, coordination behavior, and properties of Schiff base metal complexes. Elemental (CHN) analysis helps confirm the molecular composition. Spectroscopic techniques such as UV-vis spectroscopy, infrared (IR) spectroscopy, and nuclear magnetic resonance (NMR) spectroscopy are crucial for understanding the structural features and properties of Schiff bases metal complexes [22]. UV-vis spectroscopy provides information on electronic transitions, such as $\pi \rightarrow \pi^*$, $n \rightarrow \pi^*$, and d–d transitions, especially the conjugation and electronic configuration of the carbon-nitrogen double bond [39]. NMR, both proton (^1H) and carbon (^{13}C), provides detailed information about the connectivity and positioning of atoms within the molecule.

Additionally, other analytical methods, including mass spectrometry (MS) and elemental analysis, complement spectroscopic techniques by confirming molecular weight and elemental composition. Mass spectrometry confirms molecular weight and fragmentation. For paramagnetic metal centers, electron paramagnetic resonance (EPR) spectroscopy provides additional data on oxidation state and coordination environment.

Infrared (IR) spectroscopy is used to identify functional groups in organic molecules by analyzing vibrational transitions caused by radiation absorption. In Schiff bases, the presence of the characteristic C=N (imine) group is confirmed by a band typically appearing in the 1600–1700 cm^{-1} region. Upon complexation with metal ions, the C=N band shifts to a lower wavenumber, indicating coordination with the metal center. Additional bands may appear due to metal-ligand bonds such as M-N and M-O. A broad band at 3300–3600 cm^{-1} corresponds to O-H stretching, indicative of phenolic or hydroxyl groups in the Schiff base structure [31, 35,37].

Single crystal X-ray diffraction (SCXRD) is the definitive method for characterizing the structure of Schiff base metal complexes, providing accurate information about molecular and crystal structures of Schiff base metal complexes. SCXRD provides detailed information about the coordination geometry around the metal center, bond lengths and bond angles, ligand conformation and packing, hydrogen bonding and crystal system. Through crystal growth, data collection, and structure refinement, SCXRD reveals critical details such as the ligand binding mode and the crystal symmetry [39, 40].

Due to the great flexibility and diverse structures aspects of Schiff bases metal complexes, a wide range of these compounds and have been synthesized [7].

There are a variety of factors, advantages, and disadvantages to consider in choosing the most efficient approach for the synthesis of Schiff base legends and their metal complexes due to

environmental and green chemistry concerns. There are several methods and new techniques for the synthesis of Schiff bases, some of them have been reported as following:

1.3.1- The conventional heating method

The conventional heating method for synthesizing Schiff base compounds involves reacting a primary amine with a carbonyl compound (aldehyde or ketone) under reflux conditions, often in the presence of a solvent [17, 22]. This process leads to the formation of an imine bond (-C=N-) and the elimination of water [22].

A dehydrating agent may be used to enhance the reaction by removing water. While this method is simple and widely used, it may require longer reaction times and higher temperatures compared to newer techniques [14, 17, 22]. Venkatesh Rangaswamy et al 2021 were synthesized Schiff base through reacting 4-nitro-o-phenylenediamine with 5-methoxysalicylaldehyde in absolute ethanol, heating the mixture at 70°C for 6 hours with constant stirring scheme (1.2).

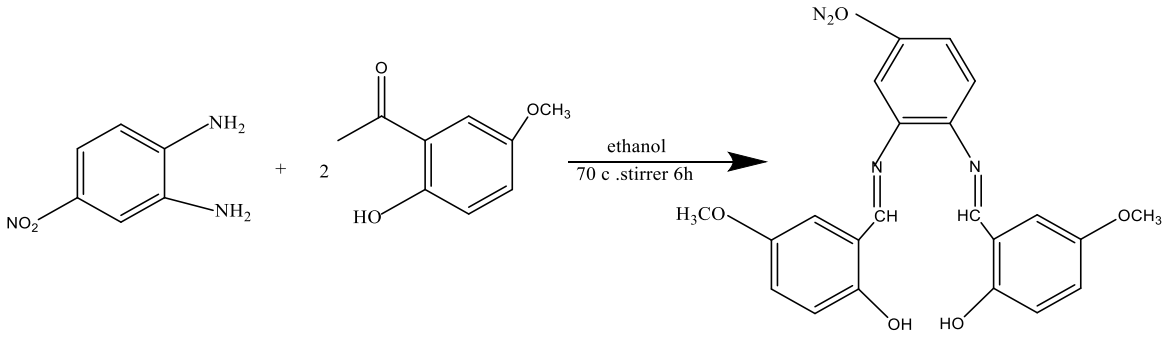

Scheme 1.2: Synthesis of Schiff base by heating method.

The synthesized Schiff base was characterized using infrared, ultra violet, molar conductance measurements and nuclear magnetic resonance spectroscopy [40]. Several techniques, including UV-vis spectroscopy, infrared spectroscopy (IR), and nuclear magnetic resonance (NMR), were used to characterize the title compound. The IR spectrum exhibited a strong absorption around 1600–1650 cm^{-1}, corresponding to the imine (C=N) stretch. A broad peak around 3200-3400 cm^{-1}, characteristic of the phenolic group. The UV-Vis spectrum displayed absorption bands between 200–300 nm, attributed to aromatic π–π* transitions, and additional bands around 300–350 nm, associated with n–π* transitions of the imine linkage. The 1H-NMR

spectra of the free ligands showed a singlet around 8–9 ppm for the imine (–CH=N) proton, aromatic protons between 6.5–8 ppm, and a signal around 10–12 ppm for the phenolic –OH group [41].

1.3.2- Modern approaches and green chemistry aspects in Schiff base synthesis

The synthesis of Schiff bases has developed significantly with the adoption of modern approaches and green chemistry principles [42]. These methods emphasize sustainability by using eco-friendly solvents like water and employing recyclable metal complexes or enzymes as catalysts, thus reducing the environmental impact [42, 43]. Microwave-assisted synthesis has become a popular energy-efficient technique, significantly shortening reaction times and improving efficiency, in accordance with green chemistry goals. Additionally, modern approaches often favor metal-free catalysis or the use of environmentally compatible metal catalysts to ensure a greener process [41, 43].

1.3.2.1- Natural acid catalyst method

The synthesis of Schiff bases using natural acid catalysts is an eco-friendly method that supports the principles of green chemistry [40- 42]. This method involves the condensation of primary amines with carbonyl compounds (aldehydes or ketones) in the presence of natural acids. Natural acids, such as citric acid, tartaric acid, lemon juice acetic acid (from vinegar), and other bio-derived acids, have been explored as catalysts for the synthesis of Schiff bases [42]. These catalysts are non-toxic, biodegradable, and readily available [42, 43]. The natural acid catalyst facilitates the formation of the imine bond (C=N) by protonating the carbonyl oxygen of the aldehyde or ketone, thus enhancing the electrophilicity of the carbonyl carbon. This enhances the reactivity toward nucleophilic attack by the amine, leading to good yields of Schiff bases. Natural acids typically work under mild conditions at room temperature or slightly higher temperatures, reducing energy consumption compared to traditional methods that involve high temperatures or strong acids [43].

1.3.2.2- Aqueous medium

Conventionally, Schiff's bases can be prepared by refluxing the amine and aldehyde in an organic solvent like ethanol or methanol, which are toxic and volatile, causing environmental harm. To reduce such disasters there is a need to use a safer reaction medium like water. Using water as a safer solvent for the condensation reaction between an amine and a carbonyl compound offers both environmental and cost benefits. Koteswara et.al (2010) has

developed eco-friendly condensation reaction method for the green synthesis of various Schiff bases, achieved by stirring 1,2-diaminobenzene with different aromatic aldehydes in water as the solvent. This method is direct, clean, and efficient, offering high yields with shorter reaction times. The product is easily purified through simple filtration, followed by washing with water and drying [44] Scheme (1.3).

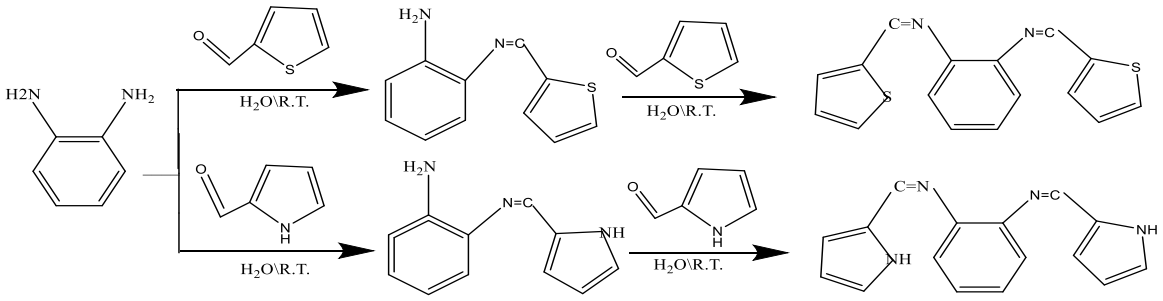

Scheme 1.3: Synthesis Schiff base by Aqueous medium

1.3.2.3 -Microwave Assistance

Microwave-assisted synthesis has become popular due to its ability to accelerate chemical reactions, enabling reactions that previously took hours or days to be completed in minutes. This method is eco-friendly, as it often requires no solvents or supporting reagents [45, 46]. It offers many benefits, including increased reaction rates, higher yields, and simpler processing. The microwave-assisted synthesis of Schiff bases involves the use of microwave radiation to speed up the condensation between an amine and a carbonyl compound (either aldehydes or ketones), leading to efficient and rapid formation of Schiff bases with improved yields and reduced reaction times compared to traditional heating methods [45- 47].

1.4 -Applications and Significance

Schiff base metal complexes are widely recognized for their versatility, ease of synthesis, diverse structures, and cost-effectiveness, making them an important focus in current chemical research [47-49]. These compounds have wide-ranging applications due to their adaptable structures, stability, and rich electronic properties.

Schiff base metal complexes exhibit a broad range of biological activities, such as antimicrobial, anticancer, antioxidant, anti-inflammatory, antimalarial, antidiabetic, and anti-Alzheimer effects [48, 49]. The majority of their bioactivity is attributed to the presence of the azomethine (C=N) group, while their adaptability results from the ability of Schiff bases to

form stable complexes with various metal ions [48, 49]. These complexes are not only significant in the biomedical field, where they show promise for therapeutic applications and combating antimicrobial resistance, but also play key roles in industrial catalysis, organic transformations, and polymerizations due to their structural stability and reactivity. Additionally, they are valuable in environmental and analytical chemistry, being used as corrosion inhibitors, metal ion sensors, and in the development of biosensors for environmental monitoring [50]. Their multifunctional nature extends to applications in clinical, analytical, and agrochemical industries, underlining their relevance across numerous scientific disciplines.

1.4.1 -Biological Activity

Many Schiff base complexes exhibit interesting biological activities including antimicrobial, anticancer, and enzyme-inhibitory properties [40, 48, 50, 51]. Several studies have demonstrated that the condensation of salicylaldehyde with various heterocyclic compounds and their derivatives [48, 50] results in products exhibiting significant antibacterial and antifungal activities. Thus, Schiff base metal complexes have gained significant attention for their enhanced antimicrobial properties, which are attributed to the synergistic effects of metal coordination and the essential reactivity of the Schiff base ligands. These complexes have demonstrated strong activity against a broad spectrum of microorganisms, including both Gram-positive and Gram-negative bacteria, as well as fungi [22, 40, 48, 51]. Copper(II) Schiff base complexes derived from antipyrine have demonstrated a broad spectrum of biological activities, including antimicrobial, anticancer, antioxidant, and anti-inflammatory effects. Their enhanced antimicrobial efficiency, when compared to the free ligands, is primarily attributed to metal chelation, which increases the complexes' lipophilicity and facilitates their penetration through microbial cell membranes [52, 53].

1.4.2- Catalysis

Schiff base metal complexes have proven to be efficient catalysts in both homogeneous and heterogeneous reactions, with their catalytic behavior strongly influenced by the metal ion, ligand structure, and coordination environment [53]. These complexes have shown effectiveness as catalysts in diverse chemical transformations such as oxidation, reduction, and polymerization, because of their ability to stabilize reactive intermediates and enhance selectivity [53]. Copper(II) Schiff base complexes, especially those derived from 4-aminoantipyrine, demonstrate strong catalytic potential in various industrial and environmental processes, owing to their structural flexibility and favorable electronic properties. Their

catalytic activity extends to environmental applications, particularly the degradation of dyes in wastewater treatment [54].

1.4.3 -Materials science

Schiff base metal complexes play a significant role in material science due to their diverse structural properties, thermal stability, and rich electronic properties. The unique optical and magnetic properties of Schiff base metal complexes have made them suitable for applications in the development of sensors, magnetic materials, and the synthesis of metal oxide nanoparticles [56, 57]. Schiff base copper complexes, particularly those derived from 4-aminoantipyrine, have emerged as valuable precursors for the synthesis of metal oxide nanoparticles, notably copper oxides (CuO, Cu_2O), These complexes decompose in a controlled manner under thermal conditions, facilitating the formation of highly pure and uniformly distributed nanoparticles without the need for external reducing or stabilizing agents [57-58]. The coordination environment provided by the Schiff base ligand plays a critical role in determining the morphology, particle size, and surface characteristics of the resulting oxides [59]. Consequently, nanoparticles synthesized from these precursors exhibit enhanced optical, electronic, photocatalytic, and antimicrobial properties, rendering them attractive for applications in photo catalysis, sensor technology, and biomedical fields [57-59].

1.5 4-Aminoantipyrine metal complex

4-Aminoantipyrine (4AAP), a pyrazole derivative (Figure 1.7) with an N-phenyl and a polar carbonyl group, is a chemically versatile compound structurally similar to N- substituted amides due to the presence of an N-phenyl group and a $–CH_2$ group next to a polar carbonyl group [54, 55]. Its high dipole moment (5.48 D) and the presence of both carbonyl and amino functional groups make it an excellent ligand for coordination with metal ions [55]. This carbonyl center and notable basicity, making it a good donor site in coordination chemistry [54,60]. It readily forms Schiff bases through condensation with aldehydes or ketones, with reactivity influenced by the electronic nature and position of substituents on the aromatic ring electron-withdrawing groups like nitro enhance coordination, while ortho-substituents may hinder activity because of steric effects [55, 60]. These Schiff bases can act as bidentate or polydentate ligands, coordinating through imine nitrogen and carbonyl or amino donor atoms, forming stable metal complexes with diverse structural and electronic properties. The coordination chemistry of 4-aminoantipyrine has been further expanded through reactions with thiocarbazides, carbazides, and several heterocyclic aldehydes, yielding a wide array of ligands [54, 55,60]. Its derivatives have been synthesized using building blocks such as aminothiazoles,

aromatic aldehydes, isatin, triazole rings, and pyrazolones, resulting in heterocyclic frameworks such as pyrazoles, pyrroles, and imidazoles. Specific Schiff bases, such as those formed with 3,4-dimethoxyphenyl or 2-hydroxy-5-methoxyphenyl substituents, have been well characterized, demonstrating the tunable nature of 4-aminoantipyrine [55]. Its tautomeric behavior, redox activity, and ability to form structurally diverse and stable metal complexes make it a valuable framework in synthetic, analytical, and coordination chemistry. Metal complexes of 4- aminoantipyrine exhibit significant potential in biological, clinical, analytical, and pharmacological applications. Due to the combined presence of the antipyrine moiety and azomethine linkage, Schiff bases and their metal complexes are of particular interest for developing new chemotherapeutic agents [55]. Studies show that these metal complexes often have higher antibacterial activity than the free Schiff bases. Various transition metal complexes, including Cu(II), Ni(II), Co(II), Mn(II), Zn(II), VO(II), Pt(IV), Au(III), and Pd(II), derived from 4-aminoantipyrine-based Schiff bases have been synthesized and evaluated for their biological activity [55, 60 - 62].

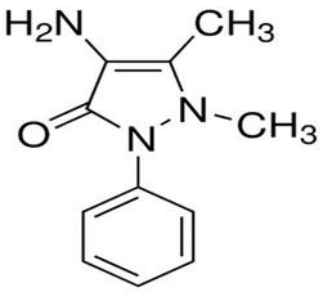

Figure 1.7: Structural formula of 4-Amino Antipyrine

1.6-Previous Studies:

Lawal and colleagues (2023) synthesized three Schiff base ligands derived from (4AAP) 4-aminoantipyrine through condensation reactions with several carbonyl compounds, including hydrazine, ethylenediamine, and benzaldehyde combined with hydrazine. These ligands were subsequently used to prepare stable copper(II) complexes in good yield. The structural features of the ligands and their corresponding metal complexes were investigated using elemental analysis, Fourier-transform infrared (FT-IR) spectroscopy, and $^{1}H/\ ^{13}C$-NMR spectroscopy. The thermal decomposition behavior of the copper complexes was also studied, revealing that the final decomposition product was copper(II) oxide (CuO).

Further morphological analysis using scanning electron microscopy (SEM) and energy dispersive X-ray spectroscopy (EDX) confirmed the formation of CuO with relatively uniform particle structures. The findings suggest that these Schiff base copper complexes possess significant thermal stability and could serve as precursors for producing nanostructured metal oxides with Potential applications in materials science [63].

The research titled "Synthesis and Characteristic Study of Co(II), Ni(II), and Cu(II) Complexes of New Schiff Base Derived from "4-Amino Antipyrine" investigates the creation and analysis of new metal complexes formed from a Schiff base ligand synthesized using 4-amino-antipyrine. The ligand was obtained through a condensation reaction and then reacted with cobalt (Co), nickel (Ni), and copper (Cu) ions, chosen for their importance in biological and catalytic systems. A range of techniques such as UV-Visible, infrared (IR), and nuclear magnetic resonance (NMR) spectroscopy were used to confirm the structures of the synthesized complexes. Their thermal stability was examined through TGA/DTA analyses, while magnetic susceptibility and conductivity tests provided insights into their electronic configurations. Results indicated that the Schiff base ligand coordinated to the metal ions either as a bidentate or tridentate donor, bonding through nitrogen and oxygen atoms. The complexes exhibited various structural geometries, including square planar and octahedral, depending on the metal ion involved. The thermal behavior confirmed the compounds' stability at elevated temperatures [64].

A. Kumar., et al (2024) synthesized Schiff base ligands by condensing 4-Aminoantipyrine with aromatic aldehydes such as salicylaldehyde and 2-hydroxy-1-naphthaldehyde, which were then complexed with transition metals including Cu(II), Co(II), Ni(II), and Zn(II) to enhance their solubility in aqueous media. Characterization of these complexes was performed using various spectroscopic techniques: FT-IR confirmed the formation of the Schiff base linkage (C=N imine stretch) and metal coordination through peak

shifts, UV-Vis spectroscopy suggested probable geometries (e.g., octahedral for Co(II) and square planar for Cu(II)), while NMR and ESI-MS verified ligand purity and complex stoichiometry. XRD analysis confirmed the crystalline nature of selected complexes, and thermal studies (TGA) demonstrated their stability up to temperatures exceeding 200°C. Water solubility of these complexes improved owing to the incorporation of polar functional groups like –OH and SO_3H into the Schiff base structure. Biological evaluations revealed significant antimicrobial activity, particularly for Zn(II) complexes, while Cu(II) complexes showed notable cytotoxicity against MCF-7 breast cancer cells. Additionally, the complexes exhibited strong antioxidant properties [65].

In the study by Kargar et. al a (2021), a series of mononuclear copper(II) complexes were synthesized using Schiff base ligands derived from the condensation of 4-aminoantipyrine with various substituted salicylaldehydes. These ligands functioned as bis-O, N-bidentate donors, coordinating through the phenolic oxygen and azomethine nitrogen atoms. The synthesized complexes were characterized using a combination of elemental analysis, FT-IR spectroscopy, and (^{1}H and ^{13}C) NMR spectroscopy. Single-crystal X-ray diffraction studies revealed that one of the complexes adopts a highly distorted square planar geometry with a 2:1 ligand-to-metal stoichiometry, where the distortion is largely influenced by the steric and electronic nature of the substituents on the salicylaldehyde moiety. The antimicrobial activity of both the ligands and their Cu(II) complexes was evaluated against Staphylococcus aureus and Escherichia coli. The results demonstrated that the copper complexes exhibited significantly higher antibacterial activity than their corresponding free ligands. This enhanced bioactivity was attributed to the metal coordination and the nature of the substituents, suggesting that structural modifications in the Schiff base structure can effectively adjust the biological properties of such complexes [66].

The study titled "Synthesis and DFT Studies of 4-Aminoantipyrine-Derived Cu(II) Schiff Base Complexes, presents the synthesis, structural characterization, and theoretical analysis of copper(II) complexes derived from Schiff bases formed by the condensation of 4-aminoantipyrine with various aldehydes. These ligands, containing both nitrogen and oxygen donor atoms, successfully coordinated with Cu(II) ions to form stable complexes. Structural elucidation was achieved through a combination of spectroscopic techniques, including UV-Vis, FT-IR, and NMR spectroscopy, confirming the successful formation of both ligands and their corresponding metal complexes. Thermal analysis using TGA revealed that the resulting complexes possessed significant thermal stability. Additionally, Density Functional Theory (DFT) calculations were performed to optimize molecular geometries and explore electronic

properties, which supported experimental observations by predicting square planar or slightly distorted square planar configurations for the Cu(II) complexes. The biological activity of these complexes was also investigated, with results indicating notable antimicrobial effects against selected bacterial strains. Overall, the findings underscore the potential of these 4-aminoantipyrine-based copper(II) Schiff base complexes in applications such as medicinal chemistry and antimicrobial drug development [67].

Hadi Kargar et al (2020) were synthesized Copper(II) complexes formed with Schiff base ligands derived from 4-aminoantipyrine. These ligands were synthesis through the condensation of 4-aminoantipyrine with various aldehydes, yielding bidentate molecules that coordinate to copper through azomethine nitrogen and carbonyl oxygen atoms. The resulting complexes were analyzed using elemental analysis, IR, UV-Vis, NMR, mass spectrometry, and single-crystal X-ray diffraction, which revealed that the copper centers adopt either square planar or distorted square pyramidal geometries. Theoretical calculations using Density Functional Theory (DFT) supported experimental data and provided further insight into electronic structures, including HOMO–LUMO energy gaps and potential reactivity. Spectroscopic studies confirmed the coordination mode and indicated ligand-to-metal charge transfer transitions. Importantly, the synthesized Cu(II) complexes exhibited notable antibacterial activity against both Gram-positive and Gram-negative bacteria, outperforming the free ligands. The study also demonstrated that the nature and position of substituents on the Schiff base ligands significantly influenced the antibacterial efficacy, suggesting that electronic effects play a key role in modulating biological activity [68].

1.7- Aim of the Study

The present study aims to synthesize a copper(II) Schiff base complex derived from the condensation of 4-aminoantipyrine with salicylaldehyde, resulting in the formation of the ligand 4-(salicylideneamino)-1,5-dimethyl-2-phenyl-1H-pyrazol-3(2H)-one. This ligand will subsequently coordinate with copper(II) chloride to form the target metal complex. The synthesized ligand and its copper(II) complex will be characterized using infrared (IR) and UV-Vis spectroscopy, molar conductivity measurements, solubility testing, and single-crystal X-ray diffraction (SCXRD). SCXRD, a key analytical technique, will be employed to elucidate the detailed molecular and crystal structure of the copper(II) complex.

CHAPTER II :
EXPERIMENTAL

2- Experimental:

2. 1-Starting Materials

List of chemicals and reagents used are given in (Table 2.1).

Table 2.1-List of chemicals and reagents used in the present study

Chemicals	Source
4-Amino antipyrine	Sigma Aldrich
Salisaldehyde	Sigma Aldrich
Ethanol	Sigma Aldrich
Toluene	Sigma Aldrich
Sodium boro hydride	BDH chemicals Ltd
Copper (II) Chloride	T-Baker Lab chemicals
Petroleum Ether	T-Baker Lab chemicals

2.2- Synthesis:

2.2.1- Synthesis of Salicyliden Amino Antipyrine (SAAP)

The Schiff base ligand was synthesized by the condensation reaction between (4AAP) 4-aminoantipyrine and salicylaldehyde. Specifically, 4-aminoantipyrine (2.033 g, 10 mmol) was dissolved in 40 mL of ethanol and stirred with 2-hydroxybenz -aldehyde (1.06 mL, 10 mmol) at room temperature for 1 hour. During the reaction, an orange color appeared, which gradually shifted to a golden yellow shade, indicating the formation of the Schiff base. The resulting yellow precipitate was filtered, dried, and recrystallized from ethanol to yield yellow crystals (2.389 g). The purity of the product was monitored by TLC using chloroform and ethanol (4:1). The melting point (M.P) of the purified compound was recorded at 198–200 °C.

2.2.2- Synthesis of the Metal Complex

The biphasic interfacial was used for the synthesis of copper(II) Schiff base complexes. In this method, ion transfer occurs between two immiscible liquid phases. Ion transfer at immiscible interfaces refers to the movement of metal ions across the boundary between two immiscible liquid phases, typically an aqueous phase containing metal salts and an organic phase containing Schiff base ligands [69].

In this experiment, the process of preparing the metal Schiff base complex involved a reaction between copper(II) chloride and a synthesized Schiff base ligand in a 1:2 molar ratio of metal to ligand. 0.15 grams of copper(II) chloride were dissolved in 50 mL of distilled water, while 0.5 grams of the ligand were dissolved in 100 mL of toluene. These two solutions were then mixed together, and the resulting biphasic mixture was stirred at room temperature for a duration of three hours. Throughout this time, the color of the aqueous layer changed from blue to brown, whereas the organic layer transitioned from light yellow to an orange-yellow. Subsequently, sodium borohydride was gradually added in portions, using a solution of 0.33 grams in 50 mL of water. This addition caused bubbling to occur, and the aqueous layer turned black, while the organic layer became dark green. As the reaction continued, both layers eventually transformed into a dark brown color. The mixture was allowed to sit undisturbed in a separating funnel overnight. On the next day, the two layers were carefully separated. The organic layer was filtered and then covered, permitting the slow development of single crystals at room temperature (0.326 g).

2.3 - Methodological Approaches and Challenge

The primary aim of this study was the synthesis of Schiff base complexes through the condensation of 4-aminoantipyrine with various aldehydes, followed by coordination with metal salts. Initial optimization of reaction conditions aimed at improving yield proved insufficient for successful complexation with nickel, copper, and zinc chlorides, despite employing strategies such as ethanol dissolution, prolonged stirring, and controlled-temperature reflux. Subsequent efforts involved the reaction of the resulting Schiff base ligands (e.g., from salicylaldehyde) with phenylenediamine in a 2:1 molar ratio using potassium carbonate as a catalyst under extended reflux with TLC monitoring; however, these attempts, along with parallel reactions using ethylenediamine, did not yield satisfactory results. Alternative approaches, including microwave-assisted synthesis and inert-atmosphere reflux followed by silica gel purification, were also ineffective, often resulting in decomposition or intractable residues. A more promising method involved a biphasic organic–aqueous system, where metal salts and ligands were dissolved in separate phases. Although initial trials employed phase-transfer catalysts such as crown ether and tetrabutylammonium hydroxide, further optimization showed these were unnecessary for successful complexation. Crystallization was achieved either through slow evaporation of the organic layer at room temperature or by layered solvent diffusion using petroleum ether and toluene, with both methods yielding isolable crystals. The challenges encountered, such as low yields, degradation under microwave conditions, and sensitivity to atmospheric exposure, highlight the complexity of Schiff base complexation and

its strong dependence on reaction parameters, while the biphasic method offers a promising pathway that warrants further refinement for improved reproducibility and crystal quality.

2.4 - IR-Spectrophotometer

The infrared (IR) spectra of the synthesized 4-(Salicylideneamino)-1,5-dimethyl-2-phenyl-1H-pyrazol-3(2H)-one Schiff base ligand and its Cu complex were recorded using a Bruker FT-IR spectrophotometer equipped with OPUS software version 7.5.18. Samples were analyzed in the solid state, and spectra were collected over the range of 4000–500 cm^{-1}. The spectral data were processed and interpreted using the OPUS software suite, and key functional group assignments were made based on standard IR absorption ranges and supported by literature references.

2.5- UV Spectroscopy

UV-Vis spectroscopic analysis was performed to investigate the electronic transitions of the synthesized Schiff base copper complex. The measurements were carried out using a double-beam UV-Visible spectrophotometer (Cary 60 UV -Vis) in the wavelength range of 190–1100 nm. The complex was dissolved in toluene**,** a non-polar solvent, and in acetonitrile, a polar solvent, at an approximate concentration of 1×10^{-4} M**.** This helps in identifying d-d transitions and charge transfer related to the ligand field [22].

2.6- Crystallography method

A suitable crystal of the complex $C_{36}H_{32}CuN_6O_4$ was mounted on X-ray diffractometer, equipped with a monochromatic MoKα radiation source (λ = 0.71073 Å). The crystal was kept at a constant temperature of 293(2) K throughout the data collection process. The data were collected in the 2θ range of 4.152° to 56.728° with a total of 76,483 reflections recorded, resulting in 7,923 independent reflections after data reduction (Rint = 0.1233, Rsigma = 0.0641). All calculations were performed using the Olex2 software [70] for structure solution and refinement. The structure was solved using the SHELXD program with Dual Space [70], and refinement was carried out using the SHELXL package [72] with CGLS minimization [73]. The final refinement yielded a goodness-of-fit on F2 of 1.047. The final R1 and wR2 values for reflections with $I \geq 2\sigma(I)$ were 0.0750 and 0.1859, respectively, while the final R1 and wR2 values for all data were 0.1187 and 0.2058. The largest positive and negative electron density peaks were found at 1.38 e/Å³ and -0.78 e/Å³, respectively.

The crystal data and structure refinement are summarized in (Table 2.2) as follows: empirical formula $C_{36}H_{32}CuN_6O_4$, formula weight 676.21, triclinic crystal system, space group P-1, unit

cell dimensions a = 10.2264(12) Å, b = 12.1948(14) Å, c = 13.8506(16) Å, α = 75.926(4)°, β = 73.069(4)°, γ = 81.503(4)°, volume = 1597.3(3) Å³, Z = 2, density (calc) = 1.406 g/cm³, and the absorption coefficient (μ) = 0.734 mm⁻¹. The F (000) value is 702.0, and the crystal size was 0.4 × 0.3 × 0.26.

Table 2.2- Crystal data and structure refinement for the copper(II) complex ($C_{36}H_{32}CuN_6O_4$)

Parameter	Value
Empirical formula	$C_{36}H_{32}CuN_6O_4$
Formula weight (g/mol)	676.21
Temperature (K)	293(2)
Crystal system	Triclinic
Space group	P-1
a (Å)	10.2264(12)
b (Å)	12.1948(14)
c (Å)	13.8506(16)
α (°)	75.926(4)
β (°)	73.069(4)
γ (°)	81.503(4)
Volume (Å³)	1597.3(3)
Z	2
Density (calc., g/cm³)	1.406
Absorption coefficient (mm⁻¹)	0.734
F(000)	702.0
Crystal size (mm³)	0.4 × 0.3 × 0.26
Radiation	MoKα (λ = 0.71073 Å)
2Θ range (°)	4.152 – 56.728
Index ranges	-13 ≤ h ≤ 13, -16 ≤ k ≤ 16, -18 ≤ l ≤ 18
Reflections collected	76,483
Independent reflections	7923 [R_{int} = 0.1233, R_{sigma} = 0.0641]
Data/restraints/parameters	7,923 / 0 / 428

CHAPTER III :
RESULT AND DISCUSSION

3- Result and Discussion:

3.1- Synthesis:

3.1.1 -Synthesis of Cu-complex of Salicylidene Amino Antipyrin

Schemes (3.1& 3.2) show the synthesis route for the copper complex $[Cu(L)_2]$. Firstly, the Schiff base ligand Salicyliden amino antipyrine, was synthesized via a condensation reaction between 4-aminoantipyrine and salicylaldehyde in ethanol at room temperature. The appearance of an orange to golden yellow color indicated the formation of the Schiff base, which was isolated as yellow crystals after filtration and recrystallization, with a melting point of 198–200 °C and a yield of 78%.

Subsequently, the corresponding copper(II) complex was prepared by reacting the Schiff base with copper(II) chloride in a 1: 2 molar ratios (metal-to-ligand) gave an air-stable dark brown solid in good yield (60%) suitable for characterization.

The successful formation of the $[Cu(L)_2]$ complex was confirmed by its solubility in the organic phase and spectroscopic analysis. This synthesis approach employed the interface between two immiscible solutions, representing a precise and efficient method for coordination compound formation. In this interfacial method, copper(II) ions from the aqueous phase undergo controlled ion transfer and coordinate with the Schiff base ligands dissolved in the organic solvent (toluene), forming lipophilic $[Cu(L)_2]$ complexes that preferentially partition into the organic phase. The ITIES offers a well-defined and tunable reaction zone, promoting selective complexation and enhancing the thermodynamic stability of the resulting products [74]. Compared to conventional aqueous-phase synthesis, this approach reduces complications such as metal ion hydrolysis or precipitation and allows better control over reaction parameters such as pH and interfacial potential [75].

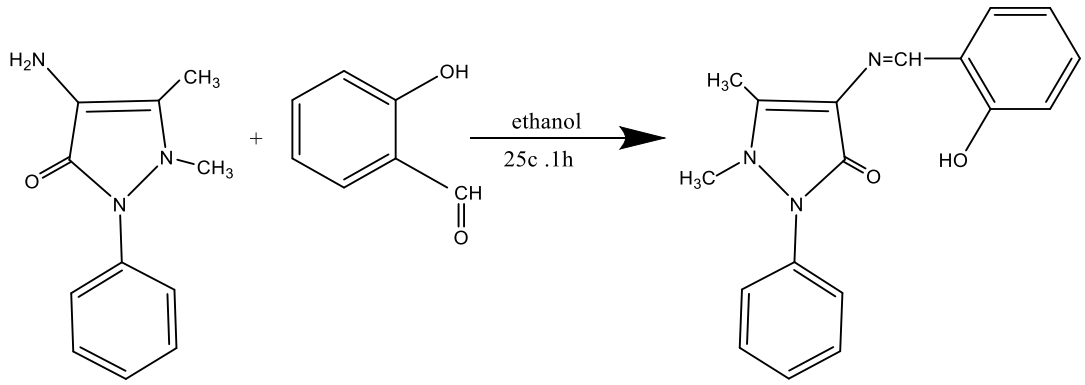

Scheme 3.1- Synthesis of ligand

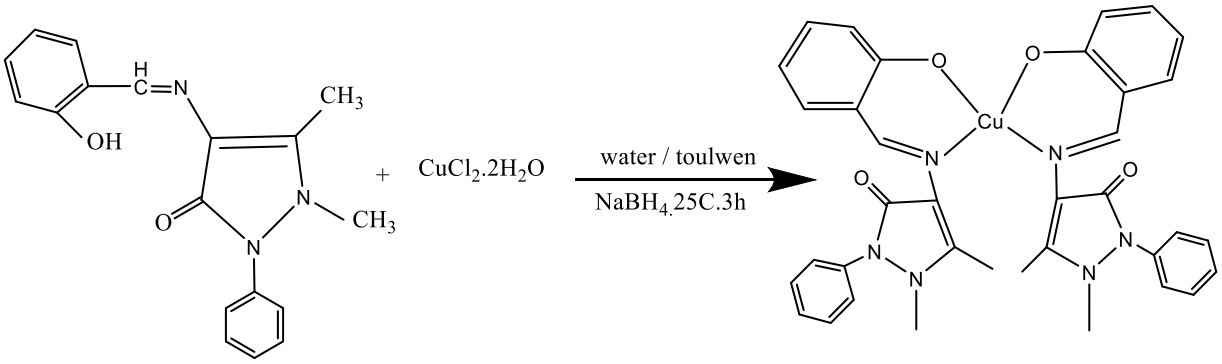

Scheme 3.2- synthesis of complex

3.2 – Solubility and Molar Conductance

The solubility of the synthesized copper(II) complex was evaluated in a range of solvents with varying polarities, including water, ethanol, methanol, acetone, benzene, dichloromethane, chloroform, petroleum ether, and diethyl ether. The complex exhibited good solubility in polar organic solvents such as ethanol, methanol, and acetone, while showing limited or no solubility in nonpolar solvents like petroleum ether and diethyl ether. This solubility behavior indicates that the complex is a neutral molecular compound, and its solubility is governed primarily by solvent polarity and compatibility with the compound's structural characteristics.

Molar conductance measurements were performed using a 1×10^{-4} M solution of the complex in chloroform at room temperature. The results showed negligible conductivity, indicating that the complex does not dissociate into free ions in solution. This non-electrolytic behavior suggests the formation of a stable, neutral, and electronically saturated coordination complex with no ionic species present in solution, further confirming its diamagnetic and non-ionic nature [22].

3.3 - FT-IR Spectroscopic Analysis

The characteristic IR frequencies (cm^{-1}) of the ligands and it complex are shown in (Table 3.1). The FT-IR spectra (Figure 3.1& 3.2) of the synthesized Schiff base ligand and its copper(II) complex were recorded to confirm the formation of the imine functional group and to investigate the coordination behavior upon complexation.

The free ligand exhibited a characteristic strong absorption band around 1590 cm^{-1}, attributable to the azomethine (C=N) stretching vibration, confirming the successful condensation of the primary amine with the aldehyde precursor. Upon complexation with Cu(II), this band shifted to a lower frequency (~1578 cm^{-1}), which is indicative of coordination of the imine nitrogen to the metal center. This shift results from the electron density donation from the nitrogen lone pair to the metal ion, which weakens the C=N bond and consequently lowers its stretching frequency [60, 66]

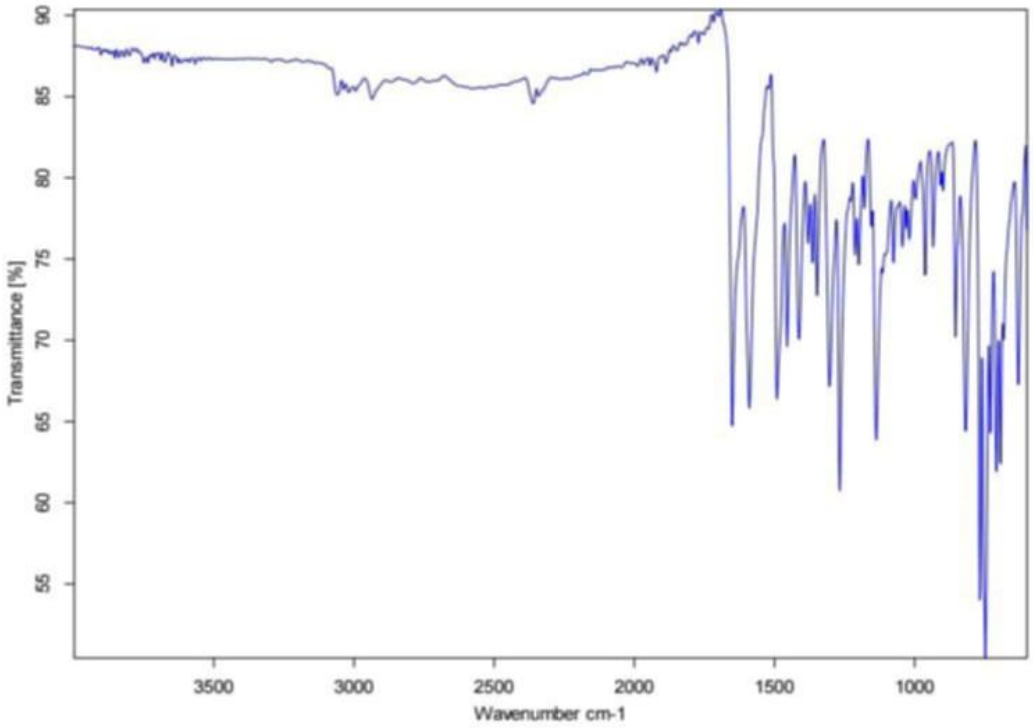

Figure 3.1: IR spectrum of the ligand

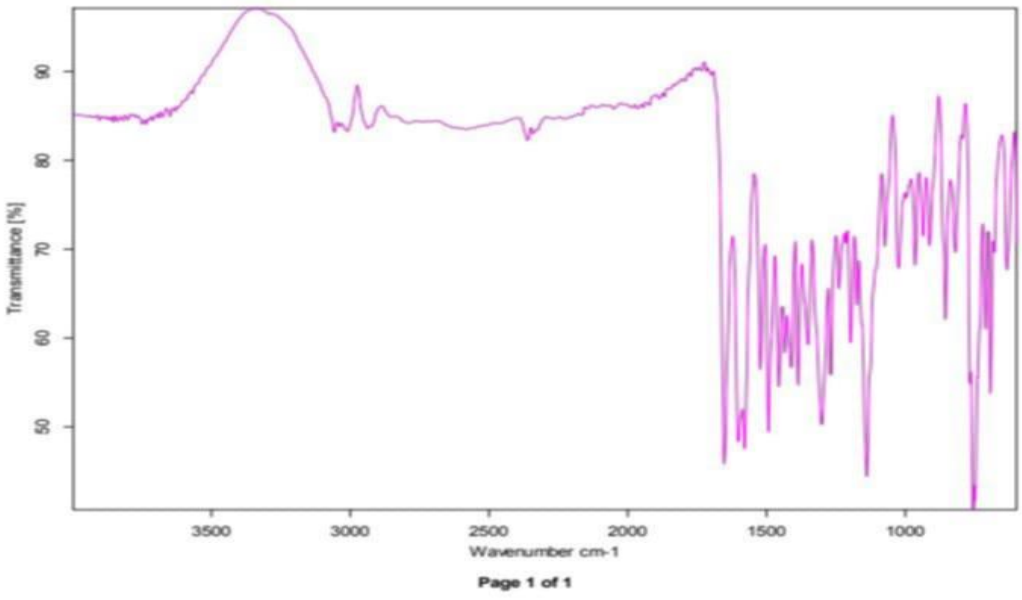

Figure 3.2: IR spectrum of the complex

Additionally, the broad band observed in the free ligand at ~3036cm^{-1}, typically assigned to O–H stretching of a phenolic group, disappeared or became significantly weaker in the spectrum of the Cu(II) complex. This suggests deprotonation and subsequent coordination of the phenolic oxygen to the metal ion. New bands appearing in the 500–600 cm^{-1} region in the spectrum of the complex can be assigned to Cu–O and Cu–N stretching vibrations, further confirming the coordination of both the azomethine nitrogen and the phenolioxygen atoms to the Cu(II) ion. The stretching frequency of the phenolate oxygen (C-O) band at 1363 cm^{-1} for Schiff base (HL) shifted to a lower frequency in complexes at 1350 cm^{-1} supports coordination through the phenolate oxygen [54, 60, 66].

The spectral changes collectively provide compelling evidence for the bidentate nature of the Schiff base ligand, coordinating through both the azomethine nitrogen and the phenolic oxygen, leading to the formation of a stable Cu(II) complex.

Table 3.1- Characteristic IR frequencies (cm^{-1}) of the ligand and its Cu(II) complex

Compound	Functional Group	Observed Band (cm^{-1})	Assignment
Schiff base ligand	C=N (azomethine)	~1590	C=N stretching
	O–H (phenol)	~3036 w	bonded OH group
	C=O (carbonyl)	~1653	C=O stretching
	C-O (phenolate)	~1363	C-O bending in plane
Cu(II) complex	C=N (azomethine)	~1578	Shifted, coordination via N
	C=O (carbonyl)	~1653	C=O stretching
	C-O (phenolate)	~1350	Shifted, coordination via O
	Cu–N / Cu–O	500-600	Metal–ligand bond vibrations

3.4- UV-vis spectroscopy

The UV-Visible spectrum of the Cu(II) Schiff base complex derived from 4-aminoantipyrine in toluene (Figure 3.3) exhibits characteristic ligand- and metal-centered transitions. Absorption bands at 321 and 346 nm are assigned to $\pi \rightarrow \pi^*$ and $n \rightarrow \pi^*$ transitions of the azomethine and aromatic moieties, respectively [56]. Broader absorptions in the 369–417 nm range correspond to intra-ligand charge transfer (ILCT) transitions, consistent with related Schiff base systems exhibiting bands at 336–360 and ~420 nm [76]. A characteristic band at 508 nm with a broad spectral feature is attributed to a d–d transition of the d^9 Cu(II) ion, indicative of a square planar geometry. The breadth of this band suggests a slight distortion from ideal planarity, probably due to ligand field effects [77]. The spectral features confirm strong metal–ligand interactions and a geometry consistent with previously reported Cu(II) Schiff base complexes [78]. This result suggests that the ligand, salicyliden amino antipyrine Schiff base, forms a complex with a copper(II) ion.

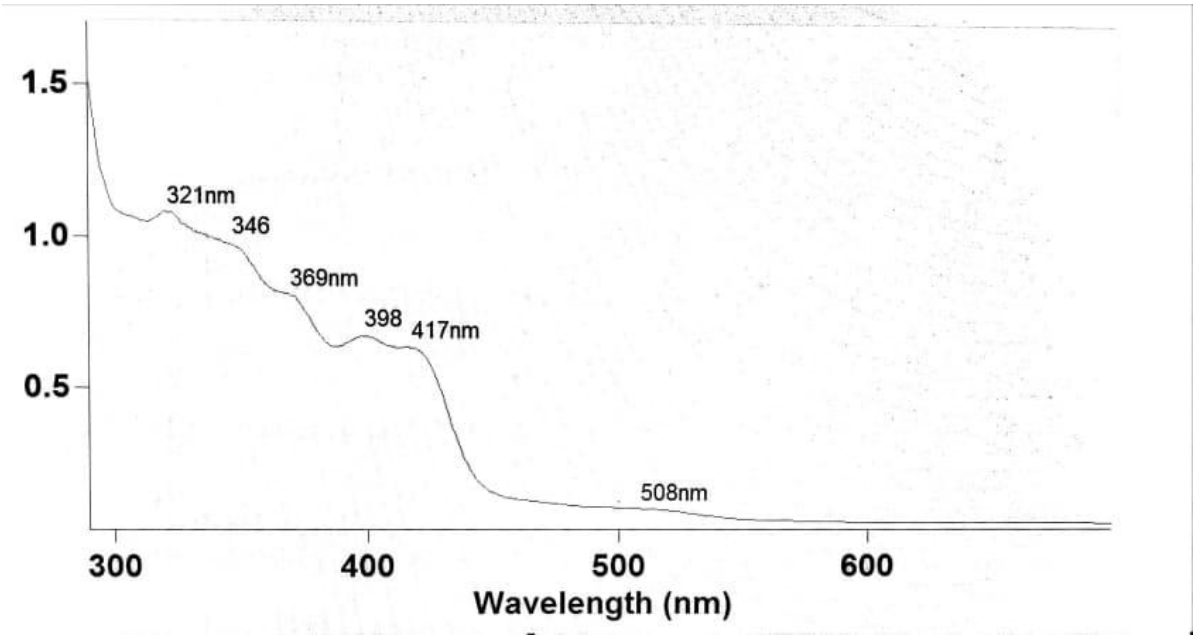

Figure 3.3: UV–Vis spectrum of Schiff base copper(II) complex in toluene solvent

The UV-Visible spectrum of the copper(II) Schiff base complex in acetonitrile (Figure3.4) reveals several distinct absorption bands that provide insight into the electronic structure and coordination environment of the complex. The UV−vis spectra of copper(II) Schiff base complex, as well as significant peaks, is shown in Figure 3.4. The spectrum displays prominent peaks at 233 nm and 273 nm, which are attributed to $\pi \rightarrow \pi^*$ electronic transitions within the aromatic rings and azomethine (C=N) group of the Schiff base ligand. A band at 316 nm is observed, corresponding to $n \rightarrow \pi^*$ transitions involving non-bonding electrons on nitrogen and

oxygen atoms, particularly from the azomethine nitrogen and phenolic oxygen [79, 80]. These transitions confirm the presence of a conjugated ligand framework and support the successful formation of the Schiff base. In the longer wavelength region, broad absorption features appear in the 396–415 nm range, which are indicative of ligand-to-metal charge transfer (LMCT) transitions [77-81]. This suggests significant electron donation from the ligand to the Cu(II) center, highlighting the strong coordination between the donor atoms and the metal ion [81]. Finally, a weaker band at 507 nm is observed and assigned to a d–d transition ($^1A_1g \rightarrow {}^1A_2g$), within the Cu(II) ion [81]. The presence of this band supports a square planar around the copper center. Overall, the spectrum in acetonitrile reflects strong solvation effects typical of polar aprotic solvents, which enhance charge-transfer transitions and stabilize excited states, leading to broader and more intense absorption bands compared to spectra recorded in non-polar solvents like toluene.

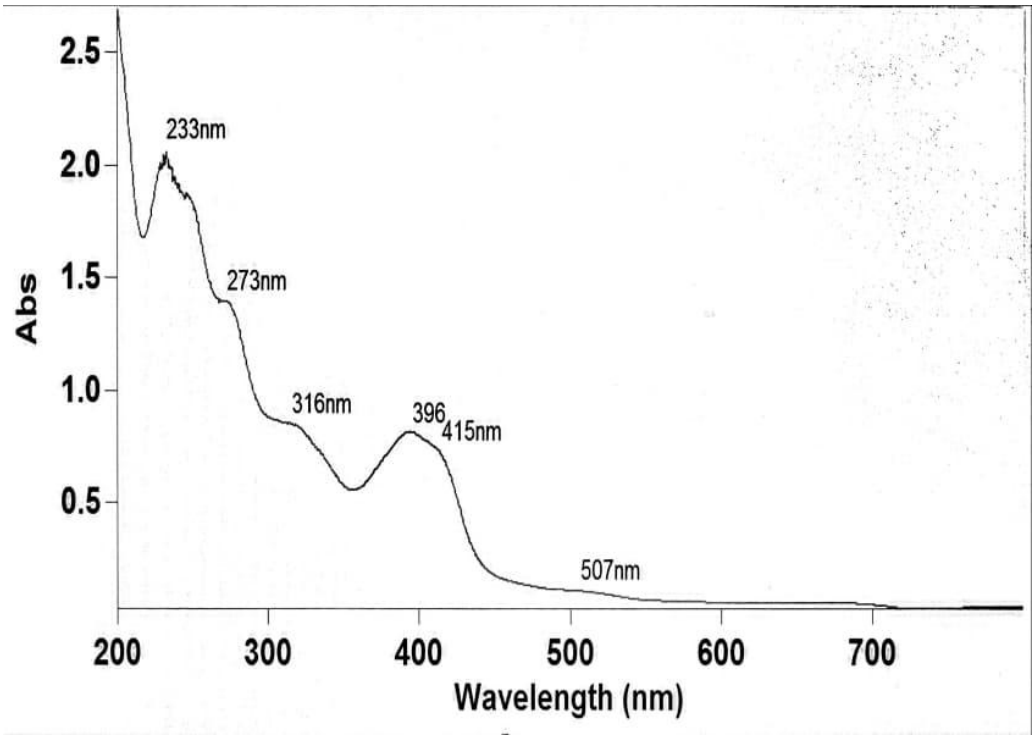

Figure 3.4: UV–Vis spectrum of Schiff base copper(II) complex in acetonitrile solvent

The electronic spectra of complex in polar and non-polar solvents are summarized in (Table 3.2). The UV-visible absorption spectra of the Salicylidene Amino antipyrine Schiff base copper(II) complex exhibit pronounced solvent-dependent behavior when measured in polar (**acetonitrile**) and nonpolar (**toluene**) solvent. In polar acetonitrile, distinct absorption bands appear at 233, 273, 316, 396, 415, and 507 nm, with high absorbance intensities reaching up to 2.5 AU. These are primarily attributed to π→π*, n→π*, and LMCT transitions, which are stabilized by the polar environment, enhancing charge-transfer character [82]. In contrast,

spectra recorded in nonpolar toluene show red-shifted and broader peaks at 321, 346, 369, 398, 417, and 508 nm, with reduced absorbance (~1.5 AU). The broader, less intense features suggest weaker solvation and possible molecular aggregation, particularly affecting d–d transitions. The observed blue shifts in acetonitrile for n→π* transitions (e.g., 321 → 316 nm) align with dipole-induced ground-state stabilization, while shifts in LMCT and π→π* bands imply specific solvent coordination effects [83]. These findings are consistent with previous reports, confirming that polar solvents enhance solute-solvent interactions, reduce aggregation, and selectively stabilize excited states [82- 85]. Overall, acetonitrile favors the observation of high-energy ligand-centered transitions, while toluene allows better resolution of lower-energy metal-centered bands. This highlights the critical role of solvent polarity in modulating the optical and electronic behavior of Schiff base copper complexes [85].

Table 3.2: Electronic absorption spectra of Schiff base complex in toluene and acetonitrile

Solvent	Absorption Peaks (nm)	Notable Transitions
Toluene	321, 346, 369, 398,417, 508	π→π*, n→π*, (ILCT), d–d (Cu^{2+})
Acetonitrile	233, 273, 316, 396, 415, 507	π→π*, n→π*, LMCT, d–d (Cu^{2+})

3.5 -X-ray crystal structure

A perspective drawing of the molecule is shown in (Figure 3.5). Selected bond lengths, angles and hydrogen-bonding interactions are summarized in (Table 3.3, Table 3.4) and (Table 3.5) respectively. The single-crystal X-ray diffraction analysis of the copper(II) complex with the molecular formula $C_{36}H_{32}CuN_6O_4$ reveals that it crystallizes in the triclinic system with space group P–1. The unit cell parameters and volume (V = 1597.3 Å^3, Z = 2) are consistent with mononuclear.

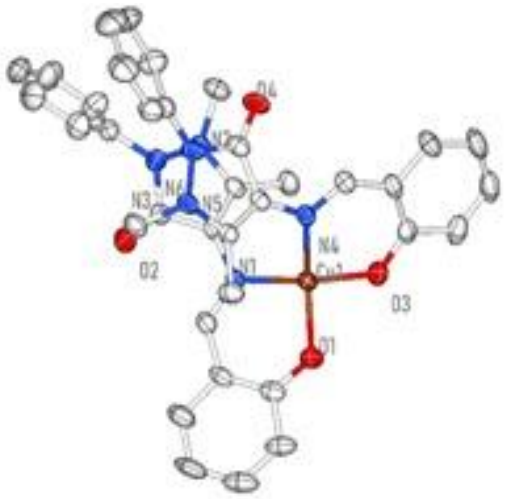

Figure 3.5; Molecular diagram of Cu(SalAAP)$_2$ complex

copper(II) complexes bearing extended Schiff base ligands. The copper center is coordinated by two nitrogen atoms and two oxygen atoms, in a *cis* orientation, resulting in a distorted square planar geometry.

From (Table 3.3), the Cu–O bond lengths are 1.903(3) and 1.886(3) Å, while the Cu–N distances are 1.971(3) and 1.968(3) Å. The shorter Cu–O bond lengths compared to Cu–N are attributed to the stronger π-donor capability of phenolic oxygen atoms, in agreement with reported values in related complexes [38, 39, 45, 49]. From (table (3. 5), angular metrics such as O1–Cu1–N4 = 144.08(13) ° and O3–Cu1–N1 = 143.35(12) ° support the distorted square planar coordination, a common feature among Schiff base Cu(II) complexes, often due to steric hindrance and ligand backbone strain [18–21, 44, 46].

The refinement indicators (R_1 = 0.0750, wR_2 = 0.2058, and goodness-of-fit = 1.047) confirm a structural model, with minor residual electron density and slightly elevated displacement parameters around outer atoms suggesting minor local disorder.

Additionally, hydrogen-bonding interactions are summarized in (Table 3.5). Several weak-to-moderate intermolecular C–H···O hydrogen bonds (D···A = 2.9–3.4 Å, angles = 113–157°) contribute to crystal packing stabilization, consistent with known non-classical interactions in Schiff base frameworks. Besides intermolecular hydrogen bonding, there are also intramolecular C–H…O interactions in the structure. For example, the methyl hydrogens H11 and H23 of different ligands interact with the ketone oxygens O4 and O2. The first interaction is C14–H11…O4, where H11···O4 = 2.39 Å, C14···O4 = 3.299(6) Å, and the bond angle is 175.1°. The second is C28–H23…O2, where H23···O2 = 2.47 Å, C28···O2 = 3.364(6) Å, and an angle of 155.3°. [41, 50].

The observed torsion angles and molecular conformation reflect the flexible nature of the ligand system, typical of Schiff base ligands containing π-conjugated backbones and mobile substituents, further confirming the structural adaptability and electronic delocalization potential of such complexes [42, 43]. As illustrated in (Figure 3.5), the crystal structure of the compound $C_{36}H_{32}CuN_6O_4$ shows a complex with a central copper(II) ion that is coordinated by two bidentate Schiff base ligands**.** The structure crystallizes in the triclinic space group P-1 with unit cell parameters a = 10.2264 Å, b = 12.1948 Å, c = 13.8506 Å, and angles α = 75.926°, β = 73.069°, and γ = 81.503°, forming a unit cell volume of 1597.3 $Å^3$. Each unit cell contains two molecules, consistent with the molecular packing shown in the (Figure 1.9), which is also consistent with the value Z = 2 reported in the crystallographic data (Table 2.2). The copper ion adopts square planar geometry, coordinated through two nitrogen atoms (N1 and N4) and two oxygen

atoms (O1 and O3) with Cu–N and Cu–O bond lengths ranging from approximately 1.886 to 1.971 Å. These donor atoms originate from two symmetrical Schiff base ligands, which are formed by the condensation of aromatic aldehydes and diamines, as evidenced by the presence of azomethine (C=N) bonds and phenolic groups (C–O). The molecular packing is stabilized by several weak intermolecular hydrogen bonds, such as C28–H···O2 and C14–H···O4, which help to reinforce the lattice and guide the arrangement of molecules within the crystal. The visualization (Figure 3.6) shows two independent molecules per unit cell arranged in alternating orientations, potentially engaging in extended hydrogen bonding [21, 44, 46]. Overall, the compound forms a well-ordered crystalline framework supported by chelation and non-covalent interactions.

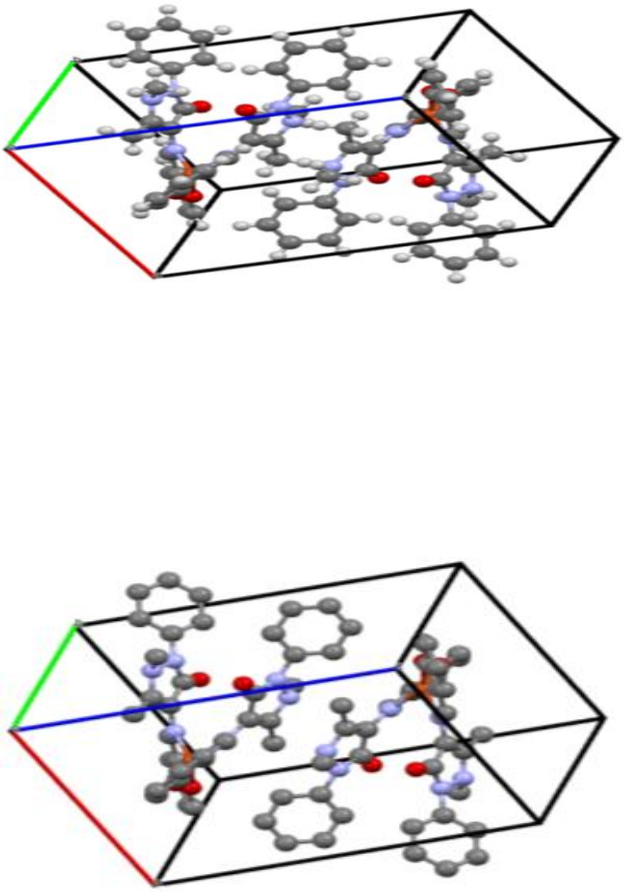

Figure 3.6: Square planar geometry for the copper(II) complex

Table 3.3- Bond Lengths

Atom	Atom	Length/Å	Atom	Atom	Length/Å
Cu1	O1	1.903(3)	C4	C13	1.446(5)
Cu1	O3	1.886(3)	C5	C6	1.494(5)
Cu1	N1	1.971(3)	C7	C8	1.362(5)
Cu1	N4	1.968(3)	C7	C12	1.373(6)
O1	C1	1.298(4)	C8	C9	1.388(6)
O2	C13	1.227(4)	C9	C10	1.365(7)
O3	C19	1.302(4)	C10	C11	1.368(7)
O4	C35	1.235(4)	C11	C12	1.375(6)
N1	C3	1.306(4)	C15	C16	1.365(6)
N1	C4	1.408(4)	C16	C17	1.389(7)
N2	N3	1.402(4)	C17	C18	1.367(7)
N2	C5	1.372(5)	C19	C20	1.424(6)
N2	C14	1.464(5)	C19	C24	1.427(5)
N3	C7	1.425(5)	C20	C21	1.422(5)
N3	C13	1.394(4)	C20	C25	1.422(5)
N4	C25	1.303(4)	C21	C22	1.371(6)
N4	C26	1.418(4)	C22	C23	1.377(7)
N5	N6	1.404(4)	C23	C24	1.372(6)
N5	C27	1.365(4)	C26	C27	1.365(5)
N5	C28	1.466(5)	C26	C35	1.442(5)
N6	C29	1.430(5)	C27	C36	1.489(5)
N6	C35	1.390(5)	C29	C30	1.381(6)
C1	C2	1.424(6)	C29	C34	1.368(6)
C1	C18	1.420(5)	C30	C31	1.391(6)
C2	C3	1.419(5)	C31	C32	1.371(8)
C2	C15	1.414(5)	C32	C33	1.376(8)
C4	C5	1.357(5)	C33	C34	1.381(6)

Table 3.4- Selected bond angles

Atom	Atom	Atom	Angle/˚	Atom	Atom	Atom	Angle/˚
O1	Cu1	N1	94.40(12)	C12	C7	N3	120.2(3)
O1	Cu1	N4	144.08(13)	C7	C8	C9	118.9(4)
O3	Cu1	O1	92.60(12)	C10	C9	C8	120.8(4)
O3	Cu1	N1	143.35(12)	C9	C10	C11	119.6(4)
O3	Cu1	N4	95.56(11)	C10	C11	C12	120.0(5)
N4	Cu1	N1	99.49(12)	C7	C12	C11	120.0(4)
C1	O1	Cu1	125.7(3)	O2	C13	N3	125.1(3)
C19	O3	Cu1	126.6(2)	O2	C13	C4	130.6(3)
C3	N1	Cu1	122.3(2)	N3	C13	C4	104.3(3)
C3	N1	C4	117.8(3)	C16	C15	C2	121.7(5)
C4	N1	Cu1	119.6(2)	C15	C16	C17	119.0(4)
C25	N4	Cu1	122.0(2)	C25	C20	C19	123.9(3)
C26	N4	Cu1	120.7(2)	C22	C21	C20	121.2(4)

(Figure 3.7) illustrates the crystal packing structure of a copper(II) Schiff base complex in the solid state, revealing a highly ordered and extended three-dimensional molecular arrangement. The atomic composition, denoted by color coding, identifies carbon (grey), hydrogen (white), copper (orange), nitrogen (blue), and oxygen (red) atoms. The copper(II) centers are clearly coordinated to nitrogen and oxygen donor atoms, most likely derived from the Schiff base ligands, forming a distorted square planar geometry, which aligns with the typical coordination preference of d^9 Cu(II) ions.

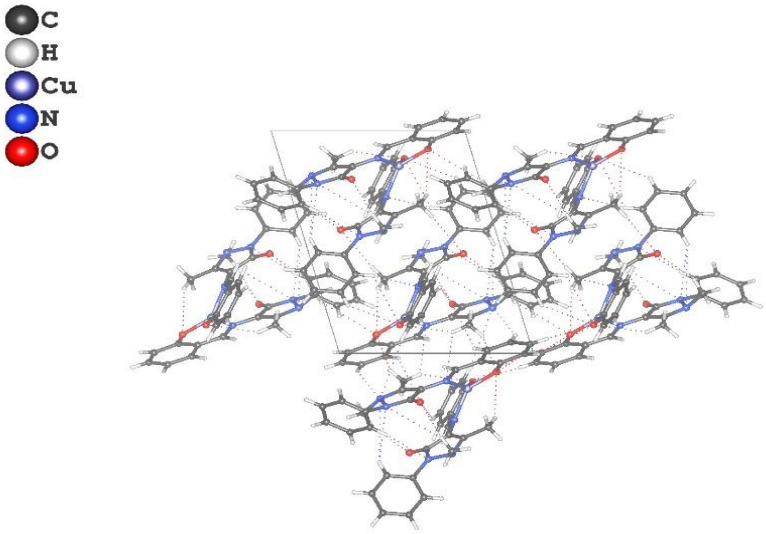

Figure 3.7: The Crystal Packing Structure of a copper(II) complex

The overall structure suggests the formation of either discrete monomeric units or polymeric chains through bridging ligands, contributing to a dense and stable crystal lattice. This extensive coordination structure is indicative of a robust supramolecular architecture, potentially stabilized through additional intermolecular interactions such as π–π stacking, hydrogen bonding, or metal-ligand bridging. Such interactions not only enhance crystal stability but also influence the material's physicochemical properties [49 -51].

Table: 3.5 - Hydrogen Bonds.

D	H	A	d(D-H)/Å	d(H-A)/Å	d(D-A)/Å	D-H-A/°
C3	H12	O2	0.93	2.43	2.971(5)	117.3
C12	H5	N1[1]	0.93	2.63	3.500(5)	155.2
C14	H11	O4	0.96	2.39	3.299(6)	157.1
C25	H21	O4	0.93	2.51	3.003(5)	113.2
C28	H23	O2	0.96	2.47	3.364(6)	155.3
C36	H32	O3[2]	0.96	2.62	3.446(5)	144.9

[1]1-X,1-Y,1-Z; 2 1-X,1-Y,2-Z

CHAPTER IV :
CONCLUSION

4 -Conclusion:

The successful synthesis and detailed characterization of a Schiff base ligand derived from 4-aminoantipyrine and salicylaldehyde, along with its corresponding copper(II) complex, have been comprehensively achieved in this study. Structural analysis, including IR spectroscopy, UV-vis spectroscopy and single-crystal X-ray diffraction, confirmed effective bidentate coordination and a distorted square planar geometry around the copper center. The biphasic synthesis method proved efficient for complex formation and crystal growth.

Based on the results of this study, it is recommended to extend the synthesis to other transition metals such as cobalt, nickel, zinc and iron in order to compare their structural features and properties. The biological activities of these compounds, particularly their potential antimicrobial and anticancer effects, should also be examined. In addition, further research could explore their catalytic applications in various reactions.

CHAPTER V:
REFERENCE AND APPENDIX

Reference

1. IUPAC. Compendium of Chemical Terminology, 2nd ed. (the "Gold Book"). Compiled by McNaught AD, Wilkinson A. Oxford: Blackwell Scientific Publications; 1997.
2. Schiff H. Mittheilungen aus dem Universitätslaboratorium in Pisa: Eine neue Reihe organischer Basen. Justus Liebigs Ann Chem. 1864;131(1):118–9.
3. Sangle SL. Introduction to Schiff base. In: Schiff base in organic, inorganic, and physical chemistry. London: IntechOpen; 2023. p. 1–13.
4. List E, Schinzer D. The Mannich Reaction in Organic Synthesis. Berlin: Springer; 2018. doi:10.1007/978-3-319-72607-7
5. Schiff H. Eine neue Reihe organischer Diamine. Zweite Abtheilung. Justus Liebigs Ann Chem. 1866;140:92–137.
6. Alam M, Alshammari A, Alharbi M, et al. Recent advances in pharmacological applications of Schiff bases and their metal complexes: A comprehensive review (2018–2023). Eur J Med Chem. 2023;250:115209. doi:10.1016/j.ejmech.2023.115209
7. Islam HM, Hannan AM. Schiff bases: Contemporary synthesis, properties, and applications. In: Novelties in Schiff bases. London: IntechOpen; 2024.
8. Kaur G, Sharma A, Banerjee B. Recent advances in Schiff base metal complexes as anticancer agents. Eur J Med Chem. 2022;232:114184. doi:10.1016/j.ejmech.2022.114184
9. Mushtaq I, Ahmad M, Saleem M, Ahmed A. Pharmaceutical significance of Schiff bases: An overview. Future J Pharm Sci. 2024;10:16.
10. Moss GP, Smith PAS, Tavernier D. Glossary of class names of organic compounds and reactivity intermediates based on structure (IUPAC Recommendations 1995). Pure Appl Chem. 1995;67(7):1307–75.
11. Uddin MN, Ahmed SS, Alam SR. Biomedical applications of Schiff base metal complexes. J Coord Chem. 2020;73(23):3109–49.
12. Li M, Cheng Z, Sun J, Tian Y, He J, Chen Y, et al. Nitrogen-doped porous carbon nanosheets based on a Schiff base reaction for high-performance lithium-ion batteries anode. Energies. 2023;16(4):1733.
13. Răzvan C, Popescu M, Ionescu S, et al. Recent advances in Schiff base ligands and their metal complexes in catalysis. Catalysts. 2024;14(4):214–235. doi:10.3390/catal14040214.

14. Das R. Schiff bases: Synthesis, applications, and characterization using FT-NMR spectroscopy. JETIR. 2018;5(1).

15. Raczuk E, Dmochowska B, Samaszko-Fiertek J, Madaj J. Different Schiff bases—Structure, importance and classification. Molecules. 2022;27(3):787.

16. John B. A review of the diverse applications of novel Schiff bases and their metal complexes. ResearchGate. 2025.

17. Subasi NT. Overview of Schiff bases. In: Schiff base in organic, inorganic, and physical chemistry. London: IntechOpen; 2022.

18. Xiao Y, Cao C. Influence of substituents on the structure of Schiff bases Cu(II) complexes. J Mol Struct. 2020;127916.

19. Meena R, Meena P, Kumari A, Sharma N, Fahmi N. Schiff bases and their metal complexes: Synthesis, structural characteristics and applications. In: Schiff base in organic, inorganic and physical chemistry. London: IntechOpen; 2023.

20. Hernández-Molina R, Mederos A. Acyclic and macrocyclic Schiff base ligands. In: McCleverty JA, Meyer TJ, editors. Comprehensive coordination chemistry II. Oxford: Elsevier; 2003. p. 411–46.

21. Boulechfar C, Ferkous H, Delimi A, Djedouani A, Kahlouche A, Boublia A, et al. Schiff bases and their metal complexes: A review on the history, synthesis, and applications. Inorg Chem Commun. 2023;150.

22. Sakhare DT. Synthesis, characterization of Schiff bases and biological activities of their transition metal complexes—Review. Int J Adv Sci Eng. 2020;6(4):1538–44.

23. Ekennia AC, Osowole AA, Olasunkanmi LO, et al. Coordination behaviors of new (bidentate N,O-chelating) Schiff bases towards copper(II) and nickel(II) metal ions: Synthesis, characterization, antimicrobial, antioxidant, and DFT studies. Res Chem Intermed. 2017;43:3787–811.

24. Akhter S, Zaman HU, Mir S, Mahmood AD, Shrivastava S. Synthesis of Schiff base metal complexes: A concise review. Eur Chem Bull. 2017;6(10):475–83.

25. Alsabra R, Radwan L. Synthesis of metal complexes Fe(II), Co(II), Ni(II) of monodentate Schiff bases derived from aromatic aldehyde. Chem Mater Res. 2016;8(7).

26. Osypiuk D, Cristóvão B, Bartyzel A. New coordination compounds of Cu(II) with Schiff base ligands—Crystal structure, thermal, and spectral investigations. Crystals. 2020;10(11):1004.

27. Jegan SJ, Muthiah PT. Synthesis, crystal structures, and supramolecular architectures of square pyramidal Cu(II) complexes containing aromatic chelating N,N′-donor ligands. Chem Cent J. 2014;8:42.

28. Maher KA, Mohammed SR. Metal complexes of Schiff base derived from salicylaldehyde—A review. Int J Curr Res Rev. 2015;7(2):1003–6.

29. Guo Y, Hu X, Zhang X, Pu X, Wang Y. The synthesis of a Cu(II) Schiff base complex using a bidentate N2O2 donor ligand: Crystal structure, photophysical properties, and antibacterial activities. Molecules. 2019;24(9):1737.

30. Yusuf TL, Oladipo SD, Zamisa S, Kumalo HM, Lawal IA, Lawal MM. Design of new Schiff-base copper(II) complexes: Synthesis, crystal structures, DFT study, and binding potency toward cytochrome P450 3A4. ACS Omega. 2021;6:13704–18.

31. Santhi S, Harikumar B, Namboori CGR. Synthesis, characterization, and spectral studies of Fe(III) and Cr(III) Schiff base complexes with acetoacetanilidepropylenediamine. Asian J Chem. 2012;24(3):1003–6.

32. 32.Santha Lakshmi S, Geetha K, Mahadevi P. Tridentate Schiff base (ONO) transition metal complexes: Synthesis, crystal structure, spectroscopic, and larvicidal studies. J Chem Sci. 2016;128(7):1113–8.

33. Munshi SJ, Jaswinder, Kaur S, Saini S, Ingle S, Kumar SB. Metal(II) chloride complexes containing a tridentate N-donor Schiff base ligand: Syntheses, structures, and antimicrobial activity. J Coord Chem. 2021;74(12):1–13.

34. Jana K, Das S, Maity T, Hossain M, Debnath SC, Samanta BC, Seth SK. Synthesis, structure, and biological properties of a Co(II) complex with tridentate Schiff base ligand. J Coord Chem. 2018;71(10):1497–509.

35. Abdallah SM, Zayed MA, Mohamed GG. Synthesis and spectroscopic characterization of new tetradentate Schiff base and its coordination compounds of NOON donor atoms and their antibacterial and antifungal activity. Arab J Chem. 2010;3(2):103–13.

36. Kargar H, Torabi V, Akbari A, et al. Synthesis, crystal structure, experimental and theoretical studies of tetradentate N2O2 Schiff base ligand and its Ni(II) and Pd(II) complexes. J Iran Chem Soc. 2019;16:1081–90.

37. Abdel-Rahman LH, Abu-Dief AM, Moustafa H, Hamdan SK. Ni(II) and Cu(II) complexes with ONNO asymmetric tetradentate Schiff base ligand: synthesis, spectroscopic

characterization, theoretical calculations, DNA interaction and antimicrobial studies. Appl Organomet Chem. 2017 Feb;31(2):e3555. doi:10.1002/aoc.3555.

38. Raman N, Kulandaisamy A, Thangaraja C. Synthesis, spectral characterization of Schiff base transition metal complexes: DNA cleavage and antimicrobial activity. Proc Indian Acad Sci (Chem Sci). 2002;114(2):183–9.

39. Fun H-K, Chantrapromma S, Bocelli G, Cantoni A, Orioli PL, Pelagatti P, et al. Synthesis, characterization and crystal structure of the Schiff base ligand N,N′-bis(salicylidene)-1,2-ethanediamine and its nickel(II) complex. J Chem Crystallogr. 2001;31:451–6.

40. Dehghani-Firouzabadi AA, Sepehri S, Notash B. Synthesis and characterization of metal complexes of a new unsymmetrical tridentate NNS Schiff base ligand: X-ray crystal structure determination of nickel(II) complex. J Chin Chem Soc. 2017;64(9):1104–10.

41. Uluçam G, Gürkan P. Synthesis and characterization of Schiff base and its Mn(III), Co(II), Ni(II), Cu(II) and Zn(II) complexes: Investigation of thermal and electrochemical behaviors. J Mol Struct. 2019;1179:236–44.

42. Abu-Dief AM, Mohamed GG. A review on versatile applications of transition metal complexes incorporating Schiff bases. Beni-Suef Univ J Basic Appl Sci. 2015;4(2):119–33.

43. Gupta KC, Sutar AK. Catalytic activities of Schiff base transition metal complexes. Coord Chem Rev. 2008;252(12–14):1420–50.

44. Singh K, Barwa MS, Tyagi P. Synthesis, characterization and biological studies of Co(II), Ni(II), Cu(II) and Zn(II) complexes with bidentate Schiff bases derived by heterocyclic ketone. Eur J Med Chem. 2006;41(1):147–53.

45. Sutradhar M, Martins LMDRS, Guedes da Silva MFC, Pombeiro AJL. Biomimetic oxidations catalyzed by bioinspired copper complexes. Coord Chem Rev. 2015;301–302:200–39.

46. Kargar H, Motedayen H, Tahir MN, Sadeghi R. New tetradentate Schiff base ligands and their Mn(III) and Fe(III) complexes: Synthesis, characterization and catalytic epoxidation of alkenes. Polyhedron. 2013;52:791–8.

47. Bhowmik P, Basak T, Patra A, Chakravorty A. Modeling molybdenum enzyme intermediates. Reactions of oxomolybdenum(VI) Schiff base complexes. Inorg Chem. 1994;33(1):127–34.

48. Rajavel R, Mohanraj K, Dharmaraja J, Anandan S, Babu RR, Srinivasan C. Design and development of Schiff base ligands and their metal complexes as antiviral agents. Bioorg Chem. 2020;101:104021.

49. Ajani OO, Obafemi CA, Nwinyi CO, Akinpelu DA. Microwave assisted synthesis and antimicrobial activity of 2,4-disubstituted quinoline Schiff bases. Bioorg Med Chem. 2010;18(2):765–71.

50. Chohan ZH, Supuran CT. Metalloantibiotics: Synthesis and antibacterial activity of cobalt(II), copper(II), nickel(II) and zinc(II) complexes with furanyl-derived sulfonamides. J Enzyme Inhib Med Chem. 2005;20(3):303–7.

51. Chee SG, Cheng FY, Ting K, Rajab NF. Potential anticancer properties of Schiff base ligands and their metal complexes: A review. Curr Med Chem. 2023;30(5):530–60.

52. Rosu T, Pasculescu S, Lazar V, Chifiriuc C, Cernat R. Copper(II) complexes with ligands derived from 4-amino-2,3-dimethyl-1-phenyl-3-pyrazolin-5-one: Synthesis and biological activity. Molecules. 2006;11(11):904–14. doi:10.3390/11110904

53. Agarwal RK, Singh L, Sharma DK. Synthesis, spectral, and biological properties of copper(II) complexes of thiosemicarbazones of Schiff bases derived from 4-aminoantipyrine and aromatic aldehydes. Bioinorg Chem Appl. 2006;2006:59509. doi:10.1155/BCA/2006/59509

54. Raman N, Raja SJ, Sakthivel A. Transition metal complexes with Schiff-base ligands: 4-aminoantipyrine based derivatives–a review. J Coord Chem. 2009;62(5):691–709. doi:10.1080/00958970802326179

55. Deshmukh P, Soni PK, Kankoriya A, Halve AK, Dixit R. 4-Aminoantipyrine: A significant tool for the synthesis of biologically active Schiff bases and metal complexes. Int J Pharm Sci Rev Res. 2015;34(1):162–70.

56. Joseph J, Nagashri K, Ayisha G, Rani B. Synthesis, characterization and antimicrobial activities of copper complexes derived from 4-aminoantipyrine derivatives. J Saudi Chem Soc. 2013;17:285–94.

57. Malik MA, O'Brien P, Motevalli M. Schiff base complexes as precursors for metal oxide nanoparticles: applications in photocatalysis. J Mater Chem A. 2023;11:1234–45. doi:10.1039/D3TA01234K

58. Sahoo SK, Sharma AK, Singh UP, Butcher RJ. Schiff base metal complexes: versatile materials for catalysis, sensing, and nanotechnology. Coord Chem Rev. 2022;452:214678. doi:10.1016/j.ccr.2022.214678

59. Jia H, Roa R, Angioletti-Uberti S, Henzler K, Ott A, Lin X, et al. Thermosensitive Cu_2O-PNIPAM core-shell nanoreactors with tunable photocatalytic activity. ACS Nano. 2016;10(9):8619–28.

60. Aljazzar SO. Capturing of the copper(II) ions by several 4-aminoantipyrine Schiff bases: Synthesis, spectroscopic analysis, and decomposition of the resulted complexes into copper(II) oxide. Bull Chem Soc Ethiop. 2024;38(2):431–43

61. Ertürk G, Sekeroglu V, Yildirim E, Dindaroglu G, Atli Sekeroglu Z. Antipyrine derived-Schiff base copper complex: Synthesis, characterization, and in vitro evaluation. Inorg Chim Acta. 2022;543:121146.

62. Jiang YZ, et al. Synthesis and Catalytic Properties of Cu^{2+} Complexes with 4-Amino-Antipyrine Schiff Bases in Dye Degradation. Key Eng Mater. 2015;671:405–11.

63. Lawal OA, Ajani AA, Garba MM, Sadiq AM. Synthesis, characterization, and thermal decomposition of copper(II) complexes with Schiff bases derived from 4-aminoantipyrine. Bull Chem Soc Ethiop. 2023;37(1).

64. Kadhim HS, Abd-Alla IQ, Hashim TJ. Synthesis and characteristic study of Co(II), Ni(II) and Cu(II) complexes of new Schiff base derived from 4-aminoantipyrine. Int J Chem Sci. 2017;15(1):107.

65. Kumar A, Sharma R, Verma P. Synthesis, characterization, and biological evaluation of water-soluble Schiff base metal complexes derived from 4-aminoantipyrine. J Mol Struct. 2024;1305:137388.

66. Kargar H, Aghaei-Meybodi F, Elahifard MR, Tahir MN, Ashfaq M, Munawar KS. Some new Cu(II) complexes containing O,N-donor Schiff base ligands derived from 4-aminoantipyrine: synthesis, characterization, crystal structure and substitution effect on antimicrobial activity. J Coord Chem. 2021;74(9–10):1534–49.

67. Kumar A, Sharma R, Verma P. Synthesis and DFT studies of 4-aminoantipyrine-derived Cu(II) Schiff base complexes. Polyhedron [Internet]. 2022 [cited 2024 Jun 20];215:116112. Available from: https://doi.org/10.1016/j.poly.2022.116112

68. Kargar H, Aghaei-Meybodi F, Behjatmanesh-Ardakani R, Elahifard MR, Torabi V, Fallah-Mehrjardi M, et al. Synthesis, crystal structure, theoretical calculation, spectroscopic, and

antibacterial activity studies of copper(II) complexes bearing bidentate Schiff base ligands derived from 4-aminoantipyrine: influence of substitutions on antibacterial activity. J Coord Chem. 2020;73(24):3484–503. doi:10.1080/00958972.2020.1838265

69. Milton CB, Xu K, Shen M. Recent advances in nanoelectrochemistry at the interface between two immiscible electrolyte solutions. Curr Opin Electrochem. 2022;34:101005. doi:10.1016/j.coelec.2022.101005.

70. Dolomanov OV, Bourhis LJ, Gildea RJ, Howard JAK, Puschmann H. OLEX2: A complete structure solution, refinement and analysis program. J Appl Crystallogr. 2009;42:339–41. doi:10.1107/S0021889808042726

71. Sheldrick GM. SHELXD: a program for solving crystal structures by direct methods. Acta Crystallogr A. 2008;64(1):112–22.

72. Sheldrick GM. Crystal structure refinement with SHELXL. Acta Crystallogr C Struct Chem. 2015;71(1):3–8. doi:10.1107/S2053229614024218

73. Björck Å. Solving linear least squares problems by Gram-Schmidt orthogonalization. BIT Numer Math. 1967;7(1):1–21. doi:10.1007/BF01934122

74. Arrigan DWM. Ion-transfer electrochemistry at arrays of nano-interfaces between immiscible electrolyte solutions. Analyst. 2004;129(12):1157-65. DOI:10.1039/B415931M.

75. Kakiuchi T, Yoshimatsu T. Electrochemical aspects of ion and electron transfer reactions at liquid/liquid interfaces. Bull Chem Soc Jpn. 2006;79(10):1477-93. DOI: 10.1246/bcj.79.1477.

76. Selvakumar PM, Suresh E, Subramanian PS. Synthesis, spectral characterization and structural investigation on some 4-aminoantipyrine containing Schiff base Cu(II) complexes and their molecular association. *Polyhedron*. 2007;26(4):749–756.

77. Raman N, Kulandaisamy A, Thangaraja C. Transition metal complexes of Schiff base ligands derived from 4-aminoantipyrine and their antimicrobial activities. *J Chem Sci*. 2002;114(6):593–600. doi:10.1007/BF02707715

78. Hathaway BJ. Copper(II) complexes: stereochemistry and bonding. *Struct Bond*. 1973; 14:49–98. doi:10.1007/BFb0116467

79. Lever ABP. *Inorganic Electronic Spectroscopy*. 2nd ed. Amsterdam: Elsevier; 1984.

80. Mohammed TP, Thennarasu AS, Jothi R, Gowrishankar S, Velusamy M, Patra S, Sankaralingam M. Investigation of the inherent characteristics of copper(II) Schiff base

complexes as antimicrobial agents. New J Chem. 2024;48:12877–92. doi:10.1039/D4NJ01271B

81. Venkatesh G, Vennila P, Kaya S, Ahmed SB, Sumathi P, Siva V, Rajendran P, Kamal C. Synthesis and Spectroscopic Characterization of Schiff Base Metal Complexes, Biological Activity, and Molecular Docking Studies. ACS Omega. 2024;9(7).

82. Bartyzel A. Synthesis, thermal behaviour and some properties of CuII complexes with N,O-donor Schiff bases. J Therm Anal Calorim. 2018;131(2):1221–36. doi:10.1007/s10973-017-6563-2

83. Haja Tar A, Alhomaidan LM, Beji L, Alnafisah AS, Kouki N, Messaoudi S, Alminderej FM, Algreiby AA, Aroua LM. Electronic and photophysical properties of copper(II) complexes: Insights into solvatochromic effects, photoreduction, and fluorescence behavior. *Results Chem*. 2025; 13:101957.

84. Hush N, Reimers J. Solvent effects on the electronic spectra of transition metal complexes. Chem Rev. 2000 Feb;100(2):775–786. doi:10.1021/cr980409v.

85. Bolukbasi O, Yilmaz A, Ceylan BI. Solvent effects on UV–Vis and FT-IR spectra of indapamide combined with DFT calculations. Chem Pap. 2019;74:1103–1111.

Appendix:

Table 1 Crystal data and structure refinement**.**

Empirical formula	$C_{36}H_{32}CuN_6O_4$
Formula weight	676.21
Temperature/K	293(2)
Crystal system	triclinic
Space group	P-1
a/Å	10.2264(12)
b/Å	12.1948(14)
c/Å	13.8506(16)
α/°	75.926(4)
β/°	73.069(4)
γ/°	81.503(4)
Volume/Å^3	1597.3(3)
Z	2
ρ_{calc}g/cm^3	1.406
μ/mm^{-1}	0.734
F(000)	702.0
Crystal size/mm^3	0.4 × 0.3 × 0.26
Radiation	MoKα (λ = 0.71073)
2Θ range for data collection/°	4.152 to 56.728
Index ranges	$-13 \leq h \leq 13$, $-16 \leq k \leq 16$, $-18 \leq l \leq 18$
Reflections collected	76483
Independent reflections	7923 [R_{int} = 0.1233, R_{sigma} = 0.0641]
Data/restraints/parameters	7923/0/428
Goodness-of-fit on F^2	1.047
Final R indexes [I>=2σ (I)]	R_1 = 0.0750, wR_2 = 0.1859
Final R indexes [all data]	R_1 = 0.1187, wR_2 = 0.2058
Largest diff. peak/hole / e Å^{-3}	1.38/-0.78

Table 2 Fractional Atomic Coordinates ($\times 10^4$) and Equivalent Isotropic Displacement Parameters ($Å^2 \times 10^3$). U_{eq} is defined as 1/3 of the trace of the orthogonalised U_{IJ} tensor.

Atom	***x***	***y***	***z***	**U(eq)**
Cu1	3966.8(4)	4879.1(3)	8411.3(3)	33.26(17)
O1	3561(3)	6345(2)	8729(2)	44.4(7)
O2	7973(3)	5179(3)	5533(2)	50.2(7)
O3	2199(3)	4439(2)	9159(2)	41.0(6)
O4	6618(3)	1428(2)	7805(3)	52.1(8)
N1	5128(3)	5418(2)	7008(2)	28.4(6)
N2	5788(3)	3290(3)	5477(2)	34.6(7)
N3	7097(3)	3667(3)	5246(2)	37.9(7)
N4	4924(3)	3373(2)	8754(2)	29.8(6)
N5	8609(3)	3408(2)	7963(2)	34.2(7)
N6	8450(3)	2467(2)	7605(3)	36.5(7)
C1	4264(4)	7216(3)	8260(3)	37.7(8)
C2	5220(4)	7308(3)	7269(3)	35.9(8)
C3	5556(4)	6435(3)	6700(3)	33.8(8)
C4	5638(3)	4657(3)	6341(2)	28.5(7)
C5	4954(4)	3861(3)	6201(3)	31.0(7)
C6	3497(4)	3589(4)	6679(3)	43.3(9)
C7	8191(4)	3372(3)	4418(3)	34.7(8)
C8	9498(4)	3220(4)	4511(3)	47.3(10)
C9	10556(4)	2921(4)	3706(4)	59.5(13)
C10	10296(5)	2768(4)	2837(4)	66.3(14)
C11	8981(5)	2940(5)	2747(4)	62.3(13)
C12	7925(4)	3244(4)	3537(3)	49.0(10)

Atom	*x*	*y*	*z*	U(eq)
C13	7030(4)	4584(3)	5699(3)	34.9(8)
C14	5745(5)	2067(3)	5609(4)	50.7(11)
C15	5909(5)	8307(3)	6820(4)	53.1(11)
C16	5737(5)	9164(3)	7335(5)	62.5(14)
C17	4816(5)	9070(4)	8307(4)	60.2(13)
C18	4077(5)	8144(3)	8752(4)	50.3(11)
C19	1857(4)	3406(3)	9564(3)	35.5(8)
C20	2817(4)	2437(3)	9635(3)	37.3(8)
C21	2330(5)	1353(4)	10136(4)	53.1(11)
C22	954(5)	1216(4)	10502(4)	61.6(13)
C23	28(5)	2152(4)	10406(3)	55.1(12)
C24	435(4)	3226(4)	9975(3)	47.5(10)
C25	4263(4)	2482(3)	9256(3)	35.2(8)
C26	6369(4)	3197(3)	8378(3)	30.1(7)
C27	7326(3)	3873(3)	8368(3)	29.8(7)
C28	9719(4)	4113(3)	7318(4)	47.7(10)
C29	9586(4)	1645(3)	7382(3)	36.6(8)
C30	9608(5)	1010(4)	6676(4)	52.9(11)
C31	10712(6)	211(4)	6456(5)	72.6(15)
C32	11766(6)	67(5)	6913(5)	74.5(16)
C33	11731(5)	717(4)	7606(5)	63.1(13)
C34	10624(4)	1492(3)	7852(3)	46.6(10)
C35	7073(4)	2260(3)	7914(3)	34.4(8)
C36	7140(4)	4952(3)	8734(3)	41.1(9)

Table 3 Anisotropic Displacement Parameters (Å2×103). The Anisotropic displacement factor exponent takes the form: -2π2[h2a*2U11+2hka*b*U12+…].

Atom	**U_{11}**	**U_{22}**	**U_{33}**	**U_{23}**	**U_{13}**	**U_{12}**
Cu	35.0(3)	26.9(2)	35.5(3)	-7.46(17)	-3.28(18)	-6.34(17)
O1	50.7(17)	34.2(14)	47.0(16)	-15.3(12)	-3.5(13)	-7.2(12)
O2	35.7(15)	55.0(17)	64.3(19)	-27.2(15)	-1.1(13)	-18.2(13)
O3	33.2(14)	41.8(14)	45.1(15)	-12.9(12)	-1.4(11)	-6.1(11)
O4	44.8(16)	36.0(14)	82(2)	-23.1(14)	-12.9(15)	-12.5(12)
N1	28.1(14)	27.1(14)	30.7(15)	-5.3(11)	-8.1(12)	-5.1(11)
N2	34.8(16)	34.9(15)	37.9(17)	-11.2(13)	-8.5(13)	-10.6(13)
N3	32.2(16)	43.7(17)	42.5(18)	-20.4(14)	-3.6(13)	-11.7(13)
N4	28.3(14)	31.2(14)	30.4(15)	-6.2(12)	-6.8(12)	-7.0(11)
N5	30.4(15)	29.9(15)	46.9(18)	-10.4(13)	-12.1(13)	-8.8(12)
N6	32.8(16)	28.4(15)	53(2)	-13.9(13)	-13.5(14)	-5.2(12)
C1	39(2)	29.6(18)	51(2)	-10.8(16)	-20.6(18)	-1.0(15)
C2	36.0(19)	22.3(16)	52(20)	-2.0(15)	-18.7(17)	-5.6(14)
C3	33.2(18)	30.5(17)	35.4(19)	-2.3(14)	-8.1(15)	-5.9(14)
C4	31.7(17)	28.6(16)	24.6(16)	-2.1(13)	-5.8(13)	-9.9(13)
C5	39.1(19)	29.5(17)	25.9(17)	-2.2(13)	-10.5(14)	-9.6(14)
C6	40(2)	50(2)	45(2)	-15.9(18)	-6.0(17)	-19.1(18)
C7	36.4(19)	32.9(18)	33.3(19)	-7.4(15)	-5.6(15)	-5.2(15)
C8	40(2)	55(2)	50(2)	-13(2)	-14.7(19)	-4.5(19)
C9	29(2)	64(3)	85(4)	-21(3)	-10(2)	-4(2)
C10	54(3)	60(3)	77(4)	-34(3)	16(3)	-13(2)
C11	67(3)	76(3)	47(3)	-33(2)	-2(2)	-9(3)

C12	40(2)	62(3)	51(3)	-24(2)	-15.4(19)	2.4(19)
C13	34.3(19)	36.1(18)	36.6(19)	-12.1(15)	-5.4(15)	-10.9(15)
C14	58(3)	35(2)	62(3)	-12.9(19)	-13(2)	-16.2(19)
C15	52(3)	28.6(19)	76(3)	-4.4(19)	-18(2)	-7.9(18)
C16	63(3)	23.8(19)	105(4)	-11(2)	-29(3)	-10.0(19)
C17	72(3)	35(2)	91(4)	-27(2)	-42(3)	3(2)
C18	60(3)	34(2)	67(3)	-24(2)	-28(2)	6.5(18)
C19	38.3(19)	46(2)	24.9(17)	-13.2(15)	-2.9(15)	-13.2(16)
C20	39(2)	39.4(19)	31.8(19)	-1.7(15)	-5.1(16)	-16.7(16)
C21	58(3)	40(2)	53(3)	0.4(19)	-2(2)	-21(2)
C22	59(3)	61(3)	58(3)	-7(2)	4(2)	-36(3)
C23	43(2)	75(3)	48(3)	-19(2)	2.9(19)	-30(2)
C24	37(2)	71(3)	37(2)	-21(2)	-2.7(17)	-13(2)
C25	35.7(19)	32.7(18)	36(2)	-3.1(15)	-10.0(16)	-6.5(15)
C26	31.5(17)	26.2(16)	32.2(18)	-1.1(13)	-11.4(14)	-3.9(13)
C27	31.9(18)	25.1(16)	33.9(18)	-2.8(13)	-13.3(14)	-3.5(13)
C28	36(2)	39(2)	68(3)	-12.7(19)	-8.6(19)	-11.3(17)
C29	32.8(19)	28.4(17)	45(2)	-3.5(15)	-8.2(16)	-3.3(14)
C30	54(3)	52(3)	59(3)	-21(2)	-19(2)	1(2)
C31	78(4)	60(3)	80(4)	-38(3)	-7(3)	5(3)
C32	53(3)	55(3)	109(5)	-29(3)	-12(3)	15(2)
C33	47(3)	45(2)	94(4)	-6(3)	-25(3)	7(2)
C34	46(2)	37(2)	57(3)	-8.3(18)	-16(2)	-2.2(17)
C35	34.6(19)	30.1(17)	41(2)	-4.9(15)	-14.3(16)	-7.1(14)
C36	42(2)	35.7(19)	53(2)	-15.3(17)	-18.5(19)	-5.0(16)

Table 4 Bond Angles.

Atom	**Atom**	**Atom**	**Angle/°**	**Atom**	**Atom**	**Atom**	**Angle/°**
O1	Cu1	N1	94.40(12)	C12	C7	N3	120.2(3)
O1	Cu1	N4	144.08(13)	C7	C8	C9	118.9(4)
O3	Cu1	O1	92.60(12)	C10	C9	C8	120.8(4)
O3	Cu1	N1	143.35(12)	C9	C10	C11	119.6(4)
O3	Cu1	N4	95.56(11)	C10	C11	C12	120.0(5)
N4	Cu1	N1	99.49(12)	C7	C12	C11	120.0(4)
C1	O1	Cu1	125.7(3)	O2	C13	N3	125.1(3)
C19	O3	Cu1	126.6(2)	O2	C13	C4	130.6(3)
C3	N1	Cu1	122.3(2)	N3	C13	C4	104.3(3)
C3	N1	C4	117.8(3)	C16	C15	C2	121.7(5)
C4	N1	Cu1	119.6(2)	C15	C16	C17	119.0(4)
N3	N2	C14	115.7(3)	C18	C17	C16	121.4(4)
C5	N2	N3	106.2(3)	C17	C18	C1	121.3(5)
C5	N2	C14	120.7(3)	O3	C19	C20	124.0(3)
N2	N3	C7	121.8(3)	O3	C19	C24	118.5(4)
C13	N3	N2	110.1(3)	C20	C19	C24	117.4(4)
C13	N3	C7	125.4(3)	C21	C20	C19	119.3(4)
C25	N4	Cu1	122.0(2)	C25	C20	C19	123.9(3)
C25	N4	C26	117.0(3)	C25	C20	C21	116.8(4)
C26	N4	Cu1	120.7(2)	C22	C21	C20	121.2(4)
N6	N5	C28	116.4(3)	C21	C22	C23	119.2(4)
C27	N5	N6	107.3(3)	C24	C23	C22	122.2(4)

Atom	**Atom**	**Atom**	**Angle/°**	**Atom**	**Atom**	**Atom**	**Angle/°**
C27	N5	C28	121.8(3)	C23	C24	C19	120.5(4)
N5	N6	C29	119.8(3)	N4	C25	C20	127.1(3)
C35	N6	N5	109.3(3)	N4	C26	C35	124.7(3)
C35	N6	C29	125.9(3)	C27	C26	N4	127.0(3)
O1	C1	C2	124.0(3)	C27	C26	C35	108.3(3)
O1	C1	C18	118.8(4)	N5	C27	C36	120.5(3)
C18	C1	C2	117.2(4)	C26	C27	N5	109.6(3)
C3	C2	C1	123.7(3)	C26	C27	C36	129.8(3)
C3	C2	C15	117.0(4)	C30	C29	N6	118.1(4)
C15	C2	C1	119.3(4)	C34	C29	N6	121.1(4)
N1	C3	C2	126.7(3)	C34	C29	C30	120.8(4)
N1	C4	C13	124.4(3)	C29	C30	C31	118.3(4)
C5	C4	N1	127.3(3)	C32	C31	C30	121.2(5)
C5	C4	C13	108.3(3)	C31	C32	C33	119.6(5)
N2	C5	C6	120.0(3)	C32	C33	C34	119.9(5)
C4	C5	N2	110.3(3)	C29	C34	C33	120.2(4)
C4	C5	C6	129.6(3)	O4	C35	N6	124.9(3)
C8	C7	N3	119.3(3)	O4	C35	C26	130.1(3)
C8	C7	C12	120.5(4)	N6	C35	C26	104.9(3)

Table 5 Torsion Angles.

A	B	C	D	Angle/°	A	B	C	D	Angle/°
Cu1	O1	C1	C2	17.7(5)	C7	N3	C13	O2	-9.3(6)
Cu1	O1	C1	C18	-162.5(3)	C7	N3	C13	C4	169.0(3)
Cu1	O3	C19	C20	9.5(5)	C7	C8	C9	C10	-0.7(7)
Cu1	O3	C19	C24	-171.1(3)	C8	C7	C12	C11	1.2(7)
Cu1	N1	C3	C2	-3.5(5)	C8	C9	C10	C11	1.7(8)
Cu1	N1	C4	C5	42.1(4)	C9	C10	C11	C12	-1.2(8)
Cu1	N1	C4	C13	-136.2(3)	C10	C11	C12	C7	-0.2(8)
Cu1	N4	C25	C20	-0.6(5)	C12	C7	C8	C9	-0.8(6)
Cu1	N4	C26	C27	45.0(5)	C13	N3	C7	C8	54.2(5)
Cu1	N4	C26	C35	-133.6(3)	C13	N3	C7	C12	-125.7(4)

Table 6 Torsion Angles.

A	A	A	A	A	A	A	A	A	A	A
Cu1	O1	C1	C2	17.7(5)		C7	N3	C13	O2	-9.3(6)
Cu1	O1	C1	C18	-162.5(3)		C7	N3	C13	C4	169.0(3)
Cu1	O3	C19	C20	9.5(5)		C7	C8	C9	C10	-0.7(7)
Cu1	O3	C19	C24	-171.1(3)		C8	C7	C12	C11	1.2(7)
Cu1	N1	C3	C2	-3.5(5)		C8	C9	C10	C11	1.7(8)
Cu1	N1	C4	C5	42.1(4)		C9	C10	C11	C12	-1.2(8)
Cu1	N1	C4	C13	-136.2(3)		C10	C11	C12	C7	-0.2(8)
Cu1	N4	C25	C20	-0.6(5)		C12	C7	C8	C9	-0.8(6)
Cu1	N4	C26	C27	45.0(5)		C13	N3	C7	C8	54.2(5)
Cu1	N4	C26	C35	-133.6(3)		C13	N3	C7	C12	-125.7(4)
O1	Cu1	O3	C19	-155.6(3)		C13	C4	C5	N2	-2.2(4)

A	A	A	A	A	A	A	A	A	A	A
O1	C1	C2	C3	-2.7(6)		C13	C4	C5	C6	-179.8(4)
O1	C1	C2	C15	178.7(4)		C14	N2	N3	C7	51.9(5)
O1	C1	C18	C17	178.2(4)		C14	N2	N3	C13	-145.9(3)
O3	C19	C20	C21	177.2(4)		C14	N2	C5	C4	141.0(4)
O3	C19	C20	C25	-1.0(6)		C14	N2	C5	C6	-41.1(5)
O3	C19	C24	C23	179.8(4)		C15	C2	C3	N1	174.0(4)
N1	Cu1	O3	C19	103.4(3)		C15	C16	C17	C18	-0.4(7)
N1	C4	C5	N2	179.3(3)		C16	C17	C18	C1	2.8(7)
N1	C4	C5	C6	1.6(6)		C18	C1	C2	C3	177.5(4)
N1	C4	C13	O2	-6.6(6)		C18	C1	C2	C15	-1.2(5)
N1	C4	C13	N3	175.3(3)		C19	C20	C21	C22	3.6(7)
N2	N3	C7	C8	-146.5(4)		C19	C20	C25	N4	-3.7(6)
N2	N3	C7	C12	33.6(5)		C20	C19	C24	C23	-0.8(6)
N2	N3	C13	O2	-170.7(4)		C20	C21	C22	C23	-1.8(7)
N2	N3	C13	C4	7.6(4)		C21	C20	C25	N4	178.1(4)
N3	N2	C5	C4	6.8(4)		C21	C22	C23	C24	-1.4(7)
N3	N2	C5	C6	-175.3(3)		C22	C23	C24	C19	2.7(7)
N3	C7	C8	C9	179.3(4)		C24	C19	C20	C21	-2.2(5)
N3	C7	C12	C11	-178.9(4)		C24	C19	C20	C25	179.6(3)
N4	Cu1	O3	C19	-10.7(3)		C25	N4	C26	C27	-140.6(4)
N4	C26	C27	N5	178.9(3)		C25	N4	C26	C35	40.9(5)
N4	C26	C27	C36	0.0(6)		C25	C20	C21	C22	-178.1(4)
N4	C26	C35	O4	-4.7(6)		C26	N4	C25	C20	-175.0(3)
N4	C26	C35	N6	176.3(3)		C27	N5	N6	C29	-164.2(3)

A	A	A	A	A	A	A	A	A	A	A
N5	N6	C29	C30	-154.7(4)		C27	N5	N6	C35	-8.0(4)
N5	N6	C29	C34	25.2(5)		C27	C26	C35	O4	176.5(4)
N5	N6	C35	O4	-172.7(4)		C27	C26	C35	N6	-2.5(4)
N5	N6	C35	C26	6.4(4)		C28	N5	N6	C29	55.5(5)
N6	N5	C27	C26	6.3(4)		C28	N5	N6	C35	-148.4(3)
N6	N5	C27	C36	-174.7(3)		C28	N5	C27	C26	144.2(4)
N6	C29	C30	C31	179.9(4)		C28	N5	C27	C36	-36.9(5)
N6	C29	C34	C33	-178.2(4)		C29	N6	C35	O4	-18.4(6)
C1	C2	C3	N1	-4.7(6)		C29	N6	C35	C26	160.7(3)
C1	C2	C15	C16	3.6(6)		C29	C30	C31	C32	-1.1(8)
C2	C1	C18	C17	-1.9(6)		C30	C29	C34	C33	1.7(6)
C2	C15	C16	C17	-2.8(7)		C30	C31	C32	C33	0.4(9)
C3	N1	C4	C5	-144.3(4)		C31	C32	C33	C34	1.3(9)
C3	N1	C4	C13	37.4(5)		C32	C33	C34	C29	-2.3(7)
C3	C2	C15	C16	-175.2(4)		C34	C29	C30	C31	0.0(7)
C4	N1	C3	C2	-176.9(3)		C35	N6	C29	C30	53.4(5)
C5	N2	N3	C7	-171.2(3)		C35	N6	C29	C34	-126.8(4)
C5	N2	N3	C13	-9.0(4)		C35	C26	C27	N5	-2.4(4)
C5	C4	C13	O2	174.8(4)		C35	C26	C27	C36	178.8(4)
C5	C4	C13	N3	-3.3(4)						

Table 7 Hydrogen Atom Coordinates ($Å \times 10^4$) and Isotropic Displacement Parameters ($Å^2 \times 10^3$).

Atom	*x*	*y*	*z*	U(eq)
H12	6141.22	6605.12	6038.88	41
H1	3062.36	3613.16	6145.57	65
H3	3021.02	4135.64	7083.4	65
H2	3472.36	2844.46	7115.16	65
H8	9678.63	3314.56	5104.72	57
H7	11454.06	2823.33	3758.58	71
H6	11009.65	2548.33	2309.39	80
H4	8800.19	2852.05	2150.74	75
H5	7031.29	3363.76	3474.29	59
H9	6315.89	1824.77	5000.43	76
H10	4818.07	1899.48	5717.49	76
H11	6071.87	1673.99	6194.73	76
H16	6494.73	8383.49	6157.49	64
H15	6229.33	9800.54	7039.4	75
H13	4699.26	9649.6	8661.48	72
H14	3438.93	8120.91	9390	60
H17	2957.95	725.96	10216.93	64
H20	648.69	499.88	10810.84	74
H18	-905.13	2052.17	10642.11	66
H19	-219.68	3841.09	9949.18	57
H21	4793.69	1801.74	9380.72	42

Atom	***x***	***y***	***z***	**U(eq)**
H22	10545.32	3636.55	7127.74	72
H24	9864.13	4625.83	7697.35	72
H23	9473.25	4539.07	6706.38	72
H29	8902.82	1113.66	6355.55	64
H28	10735.62	-232.58	5991.28	87
H27	12500.85	-466.85	6754.69	89
H25	2451.27	634.25	7907.91	76
H26	10584.47	1911.86	8339.57	56
H30	7457.98	5557.96	8158.69	62
H32	7655.5	4874.61	9229.24	62
H31	6185.21	5117.8	9051.5	62

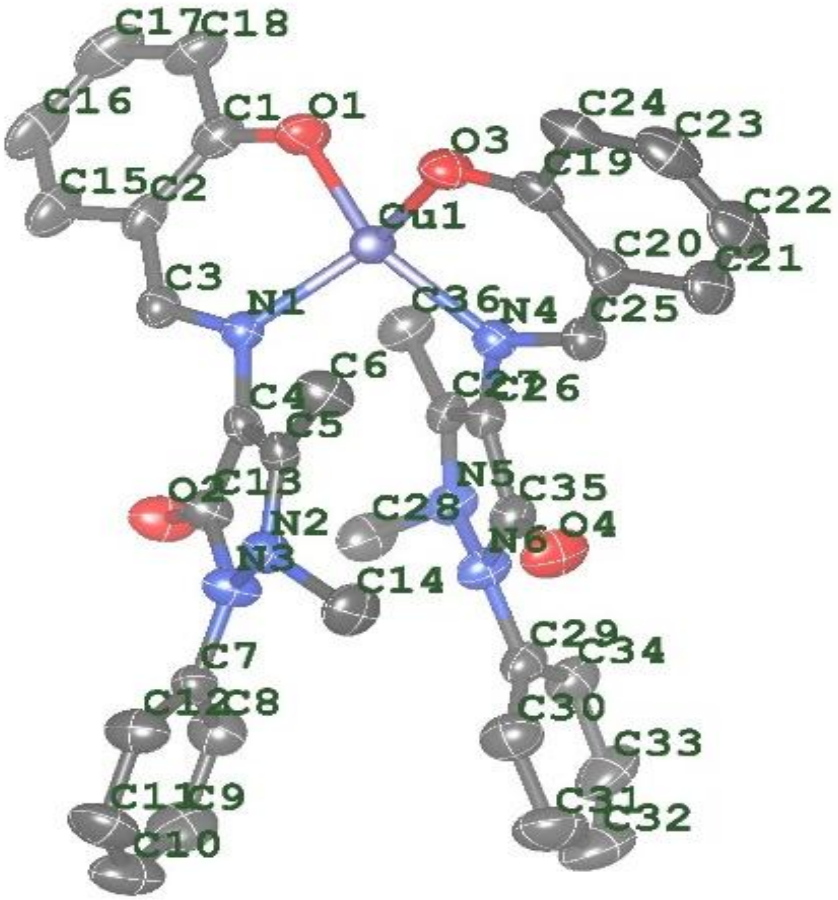

Figure 5.1: Molecular diagram of Cu(SalAAP)$_2$ complex